

ϕ -DPO: Fairness Direct Preference Optimization Approach to Continual Learning in Large Multimodal Models

Thanh-Dat Truong¹, Huu Thien Tran¹, Jackson Cothren², Bhiksha Raj³, Khoa Luu¹
¹CVIU Lab, University of Arkansas, USA ²Dep. of Geosciences, University of Arkansas, USA
³Carnegie Mellon University, USA
 {tt032, jcothre, khoaluu}@uark.edu, bhiksha@cs.cmu.edu
<http://uark-cviu.github.io/projects/Fai-DPO>

Abstract

Fairness in Continual Learning for Large Multimodal Models (LMMs) is an emerging yet underexplored challenge, particularly in the presence of imbalanced data distributions that can lead to biased model updates and sub-optimal performance across tasks. While recent continual learning studies have made progress in addressing catastrophic forgetting, the problem of fairness caused by imbalanced data remains largely underexplored. This paper presents a novel Fairness Direct Preference Optimization (FaiDPO or ϕ -DPO) framework for continual learning in LMMs. In particular, we first propose a new continual learning paradigm based on Direct Preference Optimization (DPO) to mitigate catastrophic forgetting by aligning learning with pairwise preference signals. Then, we identify the limitations of conventional DPO in imbalanced data and present a new ϕ -DPO loss that explicitly addresses distributional biases. We provide a comprehensive theoretical analysis demonstrating that our approach addresses both forgetting and data imbalance. Additionally, to enable ϕ -DPO-based continual learning, we construct pairwise preference annotations for existing benchmarks in the context of continual learning. Extensive experiments and ablation studies show the proposed ϕ -DPO achieves State-of-the-Art performance across multiple benchmarks, outperforming prior continual learning methods of LMMs.

1. Introduction

Large multimodal models (LMMs) have shown their strong performance as general-purpose assistants in various visual learning tasks [5, 19, 55, 56, 65–67]. The success of LMMs typically relies on supervised finetuning on carefully curated, large-scale multi-task datasets. In practical deployment, LMMs often suffer from performance degradation when encountering novel knowledge, tasks, or shifts in data distribution. However, fully retraining large models to incorporate new knowledge and capabilities is compu-

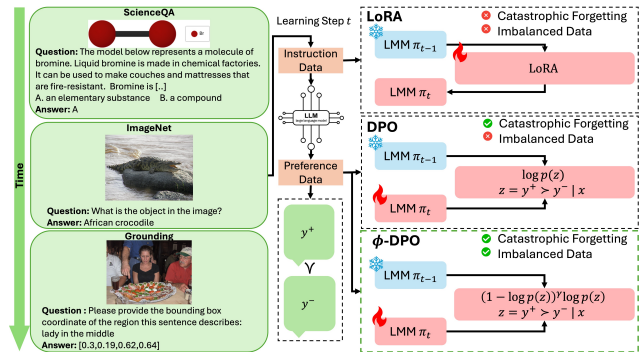


Figure 1. Our **Fairness DPO (ϕ -DPO) approach to Continual Learning in LMMs**. Prior continual learning methods, e.g., **LoRA**, struggle under **imbalanced multimodal data** and suffer from **catastrophic forgetting**. The vanilla DPO is still influenced by the **imbalanced data distributions**. Our ϕ -DPO approach can (1) mitigate forgetting, (2) adapt continuously to new learning tasks, and (3) maintain robustness under data imbalance.

tionally expensive and time-consuming. Meanwhile, direct fine-tuning on the new datasets may result in a performance drop for previously learned tasks [116]. This phenomenon is called the catastrophic forgetting problem. In addition, although recent Retrieval-Augmented Generation (RAG) improves the contextual understanding of LMMs for more accurate responses [40, 41, 87, 108], RAG-LMM systems struggle with distribution shifts and novel tasks. Since the retrieval only augments the input without updating model parameters, the internal knowledge representations remain unchanged. Therefore, to ensure the reliable performance of the LMMs in a dynamic and adaptive environment, it is crucial to develop a **Continual Learning paradigm for LMMs** (Figure 1) so that the models can incrementally acquire new information and skills while preserving the knowledge learned previously.

In continual learning, two primary challenges are identified: (1) Catastrophic Forgetting and (2) Fairness. Fairness in LMMs is particularly crucial for real-world deployment, since the biased or inconsistent behaviors can result in unequal outcomes and reduce trustworthiness, especially

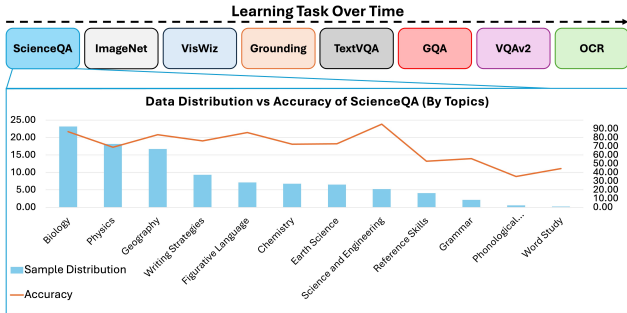


Figure 2. **The Imbalanced Distribution of Multimodal Continual Learning Benchmarks.** The distribution of samples across ScienceQA topics is highly skewed, *i.e.* categories with fewer training examples (*e.g.* Grammar, Phonological Awareness, Word Study) exhibit significantly lower accuracy, while topics with richer data (*e.g.* Biology, Physics) achieve stronger performance.

in human-centric applications. Recent studies of continual learning in LMMs [13, 116] have introduced several methods to address the catastrophic forgetting problem. However, **fairness remains a fundamental issue in the continual learning of LMMs that has been unexplored.**

As shown in Figure 2, multimodal datasets often exhibit significant topic imbalance, introducing bias during each incremental task and resulting in skewed performance. This imbalance poses two key challenges: (1) Representation Alignment and (2) Adaptability and Forgetting. Unlike traditional LMMs trained on diverse modality pairs in a single stage, continual multimodal learning proceeds sequentially, requiring incremental alignment. Under imbalanced conditions, this leads to biased gradient updates across tasks, groups, or domains (see Section 3). For example, Figure 3 illustrates the progression of training across tasks, starting with ScienceQA, which focuses on structured visual reasoning through diagram-text alignment. The subsequent Grounding task redirects attention toward object-level localization, whereas OCR-VQA centers on fine-grained text extraction. These tasks exhibit distinct visual distributions, language prompts, and alignment objectives, ultimately leading to modality imbalance and a degradation of prior representation alignment. As each task may be dominated by a particular modality or semantic class, gradient updates often favor current majority signals, undermining prior alignment and degrading performance on earlier tasks. These imbalances undermine representation alignment and may exacerbate catastrophic forgetting. Moreover, prior continual learning studies have focused on unimodal settings [10, 21, 74, 91, 94], whereas LMMs introduce new complexity due to their multimodal settings. In this context, biased data becomes a critical issue, as the imbalance in multi-modalities or semantic classes not only exaggerates catastrophic forgetting but also limits the adaptability of LMMs to new tasks or knowledge.

While data imbalance poses critical challenges, current

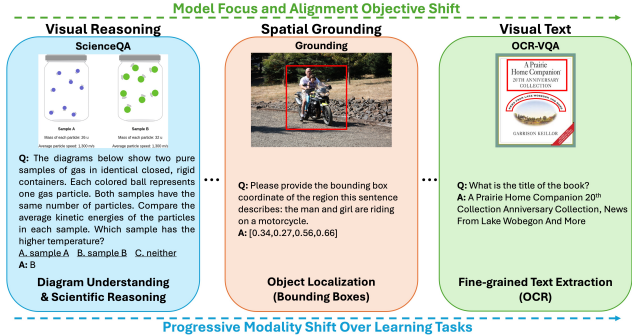


Figure 3. ScienceQA, Grounding, and OCR-VQA introduce progressively shifting visual distributions and alignment objectives, creating modality imbalance across tasks.

methods remain inadequate in addressing this problem. Low-rank Adaptation (LoRA) [36] is widely used in continual learning for LMMs [13, 26, 116]. Although it preserves the frozen backbone, its adapters can inherit dataset bias, leading to gradient updates toward majority semantic classes [12, 100]. Moreover, LoRA does not inherently mitigate bias propagation [12] and is prone to catastrophic forgetting, especially when adapters are shared or new ones induce representation drift [31, 114]. Meanwhile, Knowledge Distillation has also been widely adopted in unimodal continual learning [10, 21, 74]. However, it remains limited in multimodal contexts. LMMs often encode demographic and distributional biases from their large-scale pre-training, which distillation can transfer or amplify in the student model [81, 112]. Imitating biased teacher outputs could lead to suboptimal and biased predictions [112]. Under imbalance, majority data dominate distillation gradients, lowering generalization to tail classes [91, 94]. In addition, while distillation aligns output probabilities, it fails to preserve internal representations critical for maintaining prior knowledge, particularly in LMMs where knowledge spans multiple modalities and layers [3, 88].

Contributions. This work proposes a novel Fairness Direct Preference Optimization (FairDPO or ϕ -DPO) approach to Continual Learning in LMMs. Our contributions can be summarized as follows. First, we introduce a new continual learning paradigm, Direct Preference Optimization (DPO), which addresses the catastrophic forgetting problem in continual learning. Second, by analyzing the limitations of traditional DPO, we present a new Fairness DPO loss to address the fairness problem caused by imbalanced data. We provide a comprehensive theoretical analysis to show that our proposed approach can address both catastrophic forgetting and imbalanced data. Third, to support the DPO learning in our framework, we contribute the DPO labels for current continual learning benchmarks. Finally, our intensive experiments and ablation studies have illustrated the effectiveness and State-of-the-Art performance (SoTA) of our approach compared to prior continual learning methods.

2. Related Work

Large Multimodal Models. Early advances in large language models (LLMs) [2, 5, 17, 58, 82] have driven rapid progress in LLMs. Recent models span across vision-language [65, 67, 95], video-language [57, 61, 102, 117], and audio-language domains [24, 39], with LLMs playing a central role in scaling multimodal understanding. Early work by [4] effectively bridged vision and language modalities in a few-shot learning setting, followed by [56], which enhanced inter-modality connectivity via Q-Former. This was further developed into an instruction-aware model within the vision-language instruction-tuning framework [67]. LLaVA [67] established a streamlined visual-to-language space projection using a linear layer, later refined by [65] with an MLP and AnyRes, a technique adept at handling high-resolution images. Subsequent studies [50, 51, 54, 66, 115] contributed further improvements, culminating in a robust model [52] capable of handling diverse vision tasks. These multimodal models are finding real-world use across a variety of domains. For instance, they have been adapted for biomedical analysis [53], improved through multimodal federated learning [14], and applied to 3D point cloud understanding [64, 103, 104]. Recent work [6, 78, 98] with more effective training techniques and better architectures, serve as a stepping stone for a wide range of more advanced research efforts aimed at developing generalist LLMs.

Continual Learning. The topic of continual learning has evolved through several core paradigms, each approaching the stability-plasticity dilemma from a unique angle. The field has largely centered around rehearsal-base approaches [7, 48], regularization-based methods [47, 59, 89, 90, 93], structure-based strategies [22, 71, 92, 94], and prompt-based methods [85, 101]. In parallel, continual learning for large language models has rapidly become a focal point of recent work [79]. Depending on where adaptation occurs, current efforts can be categorized into three major stages: continual pre-training [18, 42], continual instruction tuning [76, 99, 106, 109], and continual alignment [86, 111]. Meanwhile, for LLMs, progress remains relatively limited [8, 13, 26, 28, 110, 116]. Chen *et al.* [13] introduced one of the first systematic benchmarks for continual instruction tuning of LLMs. Building on this, Zeng *et al.* [110] proposed a dual-modality guided prompt framework to improve efficiency and stability. Cao *et al.* [8] and Guo *et al.* [26] explored hierarchical and modular strategies to better preserve multimodal representations over sequential updates. Chen *et al.* [15] and Zhao *et al.* [116] further attempted to mitigate forgetting and enhance continual adaptability, while Lin *et al.* [62] proposed a novel paradigm of sparse memory fine-tuning. While prior continual learning studies in unimodal learning has taken fairness into consideration [91, 94], there are limited studies

addressing this problem in LLMs. Unlike prior methods, *we propose to address the catastrophic forgetting problem via a new continual learning paradigm and achieve fairness under imbalanced data settings.*

3. The Proposed ϕ -DPO Approach

Given a large multimodal model π , continual learning involves incrementally learning it on a sequence of datasets $\mathcal{D} = \{\mathcal{D}_1, \dots, \mathcal{D}_T\}$, where T is the number of learning steps. For each learning step t , $\mathcal{D}_t = \{x^j, y^j\}_{j=1}^{|\mathcal{D}_t|}$ constraints $|\mathcal{D}_t|$ instruction data, where $x^j = (x_{\text{img}}^j, x_{\text{ins}}^j)$ consists of a pair image (x_{img}^j) and textual instruction (x_{ins}^j), and y^j is the corresponding answer. Formally, learning the LMM π_t at step t on dataset \mathcal{D}_t can be formed as follows:

$$\pi_t^* = \operatorname{argmax}_{\pi_t} \mathbb{E}_{x,y \in \mathcal{D}_t} \log p(y|x) + D_{\text{Forget}}(\pi_t \| \pi_{t-1}) \quad (1)$$

where $\log p(y|x)$ is the supervised fine-tuning loss on the instruction data, $D_{\text{Forget}}(\pi_t \| \pi_{t-1})$ is the forgetting mitigation that prevents the current LMM π_t drifted away from the previous learned LMM π_{t-1} , *i.e.*, avoid forgetting.

Prior continual learning studies commonly adopt knowledge distillation [10, 21] to mitigate the forgetting. However, as shown in Sec. 1, the traditional knowledge distillation may exaggerate the bias and cause catastrophic forgetting, especially in the context of multimodal learning. Several recent studies adopt contrastive clustering [91, 94] to model catastrophic forgetting. Although it has yielded promising results in unimodal problems, defining clusters in multimodal settings is infeasible. Thus, to address this problem, our approach adopts Reinforcement Learning from Human Feedback (RLHF) to model the forgetting.

Formally, let $r(x, y)$ be the reward model to evaluate the forgetting and adaptability level of π_t , *i.e.*, the higher $r(x, y)$, the better memory retained and adaptability. Then, to model catastrophic forgetting (D_{Forget}), our continual learning can be reformulated under an RLHF perspective as in Eqn. (2).

$$\begin{aligned} \pi_t^* &= \operatorname{argmax}_{\pi_t} \mathbb{E}_{x \sim \mathcal{X}_t} \mathbb{E}_{y \sim \pi_t(\cdot|x)} [r(x, y)] \\ \text{s.t. } &D_{\text{KL}}(\pi_t(\cdot|x) \| \pi_{t-1}(\cdot|x)) \leq \delta, \end{aligned} \quad (2)$$

where π_{t-1} is the reference (previous learning step) policy, $D_{\text{KL}}(\pi_t \| \pi_{t-1})$ is the KL divergence to measure the difference of predictions between previous and current LLMs, δ is the threshold to constraint the policy update.

Although learning Eqn. (2) can be achieved via Proximal Policy Optimization Algorithms (PPO), it still presents two major challenges. First, learning the reward model r requires the corresponding training data. In addition, in the context of continual learning, it may require incrementally learn the reward model r at each learning step, which is not feasible. Second, learning the reward model via PPO on the imbalanced data may lead to biased predictions produced

by the model [77]. To address these challenges, inspired by [75], we propose modeling RLHF reward in continual learning via Direct Preference Optimization. We introduce a new Fairness DPO loss to address fairness modeling.

3.1. Direct Preference Optimization to Continual Learning in LMMs

3.1.1. DPO as Continual Learning

Inspired by [75], learning the LMM at learning step t of Eqn. (2) via RLHF can be rewritten using the Lagrangian multiplier as follows:

$$\pi_t^* = \max_{\pi_t} \mathbb{E}_{x, y \sim \pi_t} [r(x, y)] - \beta D_{\text{KL}}(\pi_t(\cdot | x) \| \pi_{t-1}(\cdot | x)) \quad (3)$$

where β is the Lagrangian multiplier that controls the divergence of the LMM at the current learning step from the previous step. As shown in [75], the learning objective in Eqn. (3) achieves optimal when it takes the following forms:

$$\begin{aligned} \pi_t^*(y | x) &= \frac{\pi_{t-1}(y | x) \exp\left(\frac{1}{\beta} r(x, y)\right)}{Z(x)}, \\ r(x, y) &= \beta \log \frac{\pi_t^*(y | x)}{\pi_{t-1}(y | x)} + \beta \log Z(x), \end{aligned} \quad (4)$$

where $Z(x) = \sum_y \pi_{t-1}(y | x) \exp\left(\frac{1}{\beta} r(x, y)\right)$.

From RLHF to Pairwise Preferences. In our continual learning setting, for each sample instruction data x , let y^+ be the well-retrained (good memory) and well-adapted output, and let y^- be the forgotten output. The preference of y^+ over y^- , *i.e.*, $p(y^+ \succ y^- | x)$ can be formed via the Bradley-Terry model as follows:

$$p(y^+ \succ y^- | x) = \sigma(\beta [r(x, y^+) - r(x, y^-)]), \quad (5)$$

where $\sigma(u) = \frac{1}{1 + \exp(-u)}$ is the Sigmoid function. Then, maximizing the (conditional) log-likelihood over pairs to avoid catastrophic forgetting in continual learning can be reformed as the following logistic loss:

$$\mathcal{L}_{\text{pref}}(\pi_t, \pi_{t-1}) = \mathbb{E}_{(x, y^+, y^-)} \left[-\log \sigma(\beta [r(x, y^+) - r(x, y^-)]) \right] \quad (6)$$

Continual Learning Paradigm with DPO. Under the optimum conditions defined in Eqn. (4), the logistic loss of the *reward difference* in Eqn. (6) can be written in terms of policy log-ratios as in Eqn. (7).

$$\begin{aligned} \mathcal{L}_{\text{DPO}}(\pi_t, \pi_{t-1}) &= -\mathbb{E}_{x, y^+, y^-} \left[\log \sigma \left(\beta \log \frac{\pi_t(y^+ | x)}{\pi_{t-1}(y^+ | x)} \right. \right. \\ &\quad \left. \left. - \beta \log \frac{\pi_t(y^- | x)}{\pi_{t-1}(y^- | x)} \right) \right] \\ &= -\mathbb{E}_{x, y^+, y^-} \log \sigma \left[\beta \left[\underbrace{\left(\log \pi_t(y^+ | x) - \log \pi_t(y^- | x) \right)}_{\text{trainable policy}} \right] \right. \\ &\quad \left. - \beta \left[\underbrace{\left(\log \pi_{t-1}(y^+ | x) - \log \pi_{t-1}(y^- | x) \right)}_{\text{fixed reference}} \right] \right] \end{aligned} \quad (7)$$

Interpretation. As in continual learning, each training stage aims to adapt the current policy π_t to a new learning task while preserving consistency with the reference model π_{t-1} to avoid catastrophic forgetting. The DPO objective encourages π_t to increase the relative log-odds of well-retained (or memory-consistent) y^+ over forgotten output y^- compared to π_{t-1} , effectively favoring outputs that remain aligned with prior knowledge. Our learning objective prevents the policy from drifting away from the previous learning task and implicitly regularizes updates toward the information manifold of the previous model, thereby mitigating catastrophic forgetting. Meanwhile, the hyperparameter β controls the adaptability of the LMM, *i.e.*, larger values constrain π_t to remain close to π_{t-1} (*stability*). In comparison, smaller values permit more flexible adaptation to new distributions (*plasticity*). Our learning mechanism replaces the explicit reward-based RLHF objective in Eqn. (2) with a preference-based contrastive loss that directly enforces policy consistency under a bounded divergence constraint. As a result, our DPO approach provides a principled mechanism for continual alignment, *i.e.*, preserving prior knowledge while enabling controlled updates that enhance adaptability across sequential tasks.

3.1.2. Theoretical Analysis of Direct Preference Optimization in Forgetting Mitigation

Prior studies [10, 21] have shown that Knowledge Distillation (KD) is a common approach to mitigate catastrophic forgetting. In this section, we will provide a theoretical analysis to demonstrate that the knowledge distillation loss is bounded by the DPO loss, which offers a more effective mechanism for preventing catastrophic forgetting and enhancing adaptability. In a typical knowledge distillation approach used in continual learning, the current model π_t is encouraged to remain close to the previous model π_{t-1} via the Kullback–Leibler (KL) divergence to mitigate catastrophic forgetting:

$$\mathcal{L}_{\text{KD}}(\pi_t, \pi_{t-1}) = D_{\text{KL}}(\pi_{t-1} \| \pi_t) = \mathbb{E}_{x, y \sim \pi_{t-1}} \left[\log \frac{\pi_{t-1}(y | x)}{\pi_t(y | x)} \right] \quad (8)$$

Lemma 1 Lower Bound of KL Divergence Governed by DPO Loss. *The lower bound of the $D_{\text{KL}}(\pi_{t-1} \| \pi_t)$ is governed by the DPO loss as follows:*

$$D_{\text{KL}}(\pi_{t-1} \| \pi_t) \geq \frac{1}{C_{\text{lower}}} (\log 2 - \mathcal{L}_{\text{DPO}}(\pi_t; \pi_{t-1}))^2 \quad (9)$$

where C_{lower} is a constant number.

Lemma 2 Upper Bound of KL Divergence Governed by DPO Loss. *The upper bound of the $D_{\text{KL}}(\pi_{t-1} \| \pi_t)$ is governed by the DPO loss as follows:*

$$D_{\text{KL}}(\pi_{t-1} \| \pi_t) \leq C_{\text{upper}} \mathcal{L}_{\text{DPO}}(\pi_t; \pi_{t-1}) \quad (10)$$

where C_{upper} is a constant number.

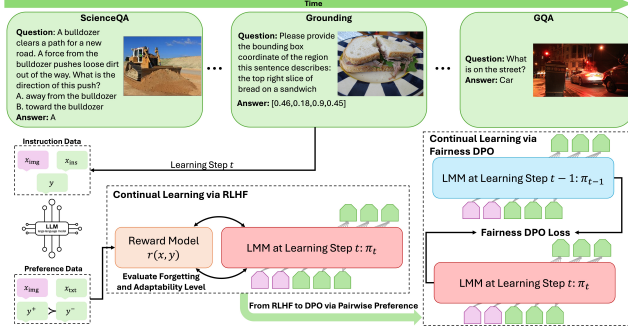


Figure 4. **Our Proposed Continual Learning Approach via Fairness DPO for Large Multimodal Models.** Traditional reinforcement learning with human feedback (RLHF) method optimizes models through explicit reward maximization. Our framework instead reformulates RLHF as Direct Preference Optimization (DPO). The Fairness DPO loss mitigate the gradient biased under the imbalanced data.

Proof. The proof of Lemmas 1-2 is in our appendix. We show the exact form of C_{lower} and C_{upper} in our proof.

Interpretation. Lemmas 1 and 2 establish a two-sided relationship between the DPO loss and the KL divergence used in prior knowledge distillation methods [10, 21]. The lower bound implies that a small DPO loss ensures π_t remains close to π_{t-1} , thereby preserving prior knowledge and mitigating catastrophic forgetting. The upper bound further constrains the KL divergence, indicating that DPO regularizes updates so that $D_{\text{KL}}(\pi_{t-1} \parallel \pi_t)$ grows proportionally to the DPO loss. These bounds indicate that DPO implicitly controls catastrophic forgetting and adaptation, *i.e.* a small \mathcal{L}_{DPO} constrains the divergence, ensuring semantic consistency with π_{t-1} while allowing new learning task updates. Different from KD, which minimizes KL divergence directly, DPO introduces an adaptive, pairwise preference mechanism. Therefore, DPO can be viewed as a generalized form of distillation, *i.e.*, retaining the regularization effect while selectively amplifying high-reward (well-retained) responses and suppressing low-reward (forgotten) ones. This makes DPO more robust to forgetting while maintaining flexibility for continual learning in LMMs.

3.2. Fairness DPO in Continual Learning

While the vanilla DPO loss can help prevent catastrophic forgetting and improve adaptability, the imbalance in data distribution can influence the behavior of DPO, leading to suboptimal performance. Indeed, let us revise the gradient produced by the DPO loss defined in Eqn. (7) as follows:

$$\begin{aligned} \nabla_{\theta} \mathcal{L}_{\text{DPO}}(\theta; \mu) &= \mathbb{E}_{\mu}[(p(z) - 1) \nabla_{\theta} s_{\theta}(z)] \\ \mathcal{L}_{\text{DPO}}(\theta; \mu) &= -\mathbb{E}_{(x, y^+, y^-) \sim \mu} [\log p(y^+ \succ y^- | x)], \end{aligned} \quad (11)$$

where θ is the parameters of LMM, $z = (x, y^+, y^-)$, and $s_{\theta}(z) = \beta(r(x, y^+) - r(x, y^-))$, μ is the data distribution of the current learning task. Let us define $p(z) = p(y^+ \succ y^- | x)$. In addition, we partition training data into K disjoint

groups $\{G_k\}_{k=1}^K$, with mixture weights $\mu_k = \mu(G_k)$. Then, the group gradients can be rewritten as follows:

$$\begin{aligned} \nabla_{\theta} \mathcal{L}_{\text{DPO}}(\theta; \mu) &= \sum_{k=1}^K \mu_k m_k(\theta) \\ m_k(\theta) &= \mathbb{E}[(p(z) - 1) \nabla_{\theta} s_{\theta}(z) \mid z \in G_k] \end{aligned} \quad (12)$$

where $m_k(\theta)$ is the group mean gradient. Let $q' = (q'_1, \dots, q'_K)$ be the desired (ideal) balanced mixture over groups, and $q = (q_1, \dots, q_K)$ the observed imbalanced distribution, with $p \neq q$. In an ideal scenario, the LLM π_t trained on the balanced data distribution q' will perform fairly. Then, the gradient difference incurred when optimizing with biased distribution q instead of balanced distribution q' can be defined as:

$$B(\theta) = \nabla_{\theta} \mathcal{L}_{\text{DPO}}(\theta; q) - \nabla_{\theta} \mathcal{L}_{\text{DPO}}(\theta; q') = \sum_{k=1}^K (q_k - q'_k) m_k(\theta) \quad (13)$$

Then, suppose there exists a group j such that $q_j > q'_j$ (major group), the j -th group contributes $(q_j - q'_j) m_j(\theta)$ in the gradient updates, which is a systematic overweighting of group j 's gradient. Meanwhile, if $q_i < q'_i$ for a minority group i , then the i -th term is underweighted. In other words, the gradient updates produced by the vanilla DPO loss will be biased towards major groups, and the gradient difference between ideal and practical data distribution will not be identical, *i.e.*, $\|B(\theta)\| \neq 0$.

To address the problem caused by the imbalanced data distribution, inspired by the focal loss [63], we introduce a new Fair DPO loss to improve the fairness of the LMM. In particular, the **Fair DPO loss** can be defined as follows:

$$\mathcal{L}_{\text{DPO}}^{\gamma}(\theta; \mu) = -\mathbb{E}_{z \sim \mu} [(1 - p(z))^{\gamma} \log p(z)] \quad (14)$$

where γ is the focusing parameter. Then, the gradient updates in Eqn. (12) can be rewritten as follows:

$$\begin{aligned} \nabla_{\theta} \mathcal{L}_{\text{DPO}}^{\gamma}(\theta; \mu) &= \sum_{k=1}^K \mu_k w_k^{\gamma}(\theta) m_k(\theta) \\ \text{where } w_k^{\gamma}(\theta) &= \mathbb{E}[\alpha_{\gamma}(p(z)) \mid z \in G_k] \\ \text{and } \alpha_{\gamma}(p) &= (1 - p)^{\gamma-1} [(1 - p) + \gamma p \log p] \end{aligned} \quad (15)$$

In Eqn. (15), $w_k^{\gamma}(\theta)$ plays a role as a modulating factor to balance the gradients of each group. Then, the gradient difference in Eqn. (13) with respect to the Fair DPO loss can be rewritten as:

$$\begin{aligned} B_{\gamma}(\theta) &= \nabla_{\theta} \mathcal{L}_{\text{DPO}}^{\gamma}(\theta; q) - \nabla_{\theta} \mathcal{L}_{\text{DPO}}^{\gamma}(\theta; q') \\ &= \sum_{k=1}^K (q_k - q'_k) w_k^{\gamma}(\theta) m_k(\theta) \end{aligned} \quad (16)$$

Lemma 3 Balanced Gradient Update of Fair DPO Loss. *Given a sufficient large value of γ , the Fair DPO loss will produce the balanced gradient update across groups regardless of the biased data distribution, *i.e.* $\lim_{\gamma \rightarrow \infty} \|B_{\gamma}(\theta)\| = 0$.*

Proof. The proof of Lemma 3 is included in our appendix.

Interpretation. When the focusing parameter γ becomes sufficiently large, the discrepancy between optimization over the imbalanced distribution and the idealized balanced distribution vanishes, *i.e.*, $\lim_{\gamma \rightarrow \infty} B_\gamma(\theta) = 0$. This indicates that our proposed Fair DPO loss can yield fairer gradient updates as γ increases. However, excessively large values of γ can cause gradient vanishing, leading to a numerically flat loss landscape. As a result, this limits the adaptability of the LMMs in continual learning settings. Meanwhile, if γ is too small, the loss behaves similarly to the standard DPO objective, potentially reinforcing the unfairness induced by imbalanced data. Therefore, careful tuning of γ is crucial to strike a balance between fairness and plasticity in the continual learning of LMMs.

Continual Learning Procedure. Figure 4 illustrates our continual learning framework. In particular, the final learning objective of our proposed approach at each learning step t can be formed as follows:

$$\pi_t^* = \operatorname{argmin}_{\pi_t} \mathbb{E}_{x,y \in \mathcal{D}_t} - \log p(y|x) + \mathcal{L}_{\text{DPO}}^\gamma(\pi_t || \pi_{t-1}) \quad (17)$$

To avoid the overfitting on small-scale size data and increase the memory-efficiency during training DPO, the LMM π_t at learning step t is optimized via LoRA.

3.3. DPO Data in Continual Learning Benchmark

We conduct our experiments on three benchmark suites: CoIN [13], MLLM-CL Domain [116], and MLLM-CL Ability [116]. The CoIN benchmark comprises eight diverse learning tasks: ScienceQA [70], TextVQA [84], ImageNet [20], GQA [38], VizWiz [30], Grounding [44, 72], VQAv2 [25], and OCR-VQA [73]. The MLLM-CL Domain benchmark is designed for domain-incremental learning and consists of five sequential domains: Remote Sensing [69], Medical [33], Autonomous Driving [83], Science [11, 29, 45, 46], and Finance [116]. The MLLM-CL Ability benchmark focuses on task-incremental learning and includes four tasks: OCR [60, 68], Math and Logic [80, 113], Visual Perception [1, 43], and GUI Agent [35, 96, 107].

While these benchmarks provide instruction-following data suitable for training LMMs, they lack pairwise prefer-

ence annotations required for DPO. To address this gap and enable continual learning via DPO, we construct pairwise preference data for each dataset within these three benchmarks. In particular, for each instruction instance, we treat the provided reference answer as the preferred output y^+ , which represents a well-retained (good-memory) and well-adapted response. To simulate the less preferred (forgotten) output y^- , we prompt a large language model to hallucinate an alternative response. The model is conditioned on both the textual instruction and the reference answer y^+ , and is instructed to generate an output y^- that is plausible and coherent, yet distinct from y^+ and potentially flawed in subtle ways. This design encourages the formation of challenging preference pairs suitable for effective DPO training. Finally, all labels are manually verified by human annotators to ensure that the rejected responses accurately reflect undesirable or suboptimal behavior (Figure 5).

4. Experimental Results

4.1. Benchmarks, Metrics, and Implementation

Benchmark and Metrics. We evaluate on three benchmarks: CoIN, MLLM-CL Domain, and MLLM-CL Ability. Following standard protocols [13, 26, 116], continual learning performance is measured using five metrics. **Last Accuracy** reports accuracy on all seen tasks after learning the final one. **Mean Finetune Accuracy** (MFT) reflects accuracy on each task immediately after learning, serving as an upper bound without forgetting. **Mean Final Accuracy** (MFN) averages accuracy across all tasks after full training. **Mean Average Accuracy** (MAA) captures the average performance over all tasks after each step. **Backward Transfer** (BWT) quantifies forgetting by comparing final accuracy to post-learning accuracy for each task. Higher scores indicate better performance.

Implementation. Our framework adopts the implementation of LLaVA v1.5 [65], using CLIP-ViT-L-14 (336^2) as the vision encoder and Vicuna 7B [17] as the language backbone. For fair comparison, we follow the training setup of [13, 26, 116], with LoRA rank 32, AdamW optimizer, a cosine learning rate schedule (base LR: $2e-5$), and batch

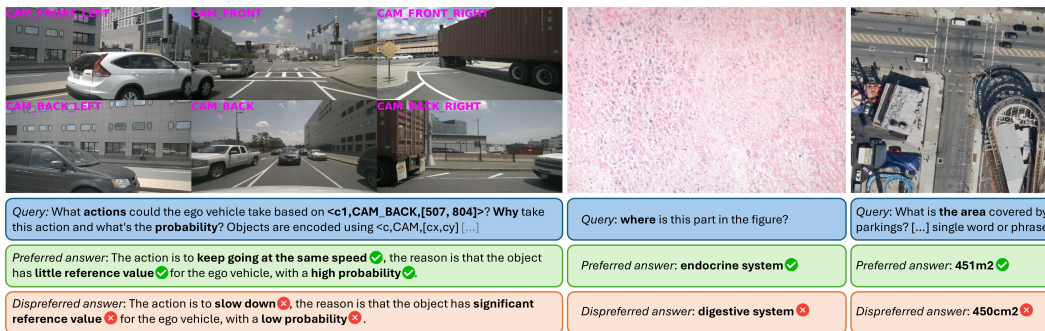


Figure 5. Example of Our DPO Data in the Continual Learning Benchmark. Best viewed in color.

Table 1. Results on MLLM-CL Domain (* denote the method using relay data). RS: Remote Sensing, Med: Medical, AD: Autonomous Driving, Sci: ScienceQA, Fin: Finance.

Method	RS	Med	AD	Sci	Fin	MFT↑	MFN↑	MAA↑	BWT↑
Zeroshot	32.29	28.28	15.59	35.55	62.56	34.85	—	—	—
LoRA-FT* [36]	76.54	50.27	43.01	43.32	89.85	66.32	60.60	64.72	-7.15
O-LoRA* [99]	76.94	41.17	34.18	39.61	83.22	60.49	55.02	60.73	-6.83
MoELoRA* [13]	77.63	49.54	39.08	41.04	89.21	66.24	59.30	64.81	-8.68
CL-MoE* [37]	76.58	52.31	39.65	45.64	90.21	66.65	60.88	64.95	-7.22
HiDe* [26]	74.80	42.29	34.03	38.01	79.22	60.83	53.67	61.81	-8.95
SEFE* [15]	78.43	52.85	46.21	47.76	89.33	66.89	62.92	66.51	-4.97
DISCO* [27]	77.78	46.25	50.45	49.51	89.71	65.27	62.74	64.92	-3.17
LoRA-FT [36]	69.65	41.59	25.43	40.88	87.45	64.98	53.00	61.13	-14.97
O-LoRA [99]	74.64	44.42	30.02	41.47	87.15	65.16	55.54	62.12	-12.03
MoELoRA [13]	77.54	41.85	27.62	40.13	86.75	64.94	54.78	61.76	-12.70
CL-MoE [37]	71.34	46.84	26.33	41.17	88.74	66.06	54.88	61.79	-13.96
HiDe [26]	74.31	48.95	33.21	38.54	81.55	60.77	55.31	60.68	-6.82
SEFE [15]	77.26	50.37	37.21	40.87	86.82	65.01	58.51	63.63	-8.13
DISCO [27]	76.03	45.20	43.79	42.33	88.95	64.43	59.26	63.35	-6.46
MR-LoRA [116]	80.87	65.32	54.12	56.71	91.12	69.64	69.63	71.06	-0.01
ϕ -DPO	85.68	69.74	57.73	61.55	95.28	74.29	74.00	75.68	-0.37

size 64 for one training epoch. All experiments are run on 16 NVIDIA A100 40GB GPUs.

4.2. Main Results

Results on the MLLM-CL Domain Benchmark. Table 1 shows results on the MLLM-CL Domain benchmark across five incremental domains: Remote Sensing (RS), Medical, Autonomous Driving (AD), Science, and Finance. Our ϕ -DPO achieves consistently outperforms prior methods in both individual accuracy (on last step) and continual learning metrics. In particular, ϕ -DPO achieves 85.58% on RS, 95.28% on Finance, and shows similar improvements on Medical (69.74%), AD (57.75%), and Science (61.55%). The results has indicated the robustness of our ϕ -DPO under domain shifts. In terms of continual learning performance, ϕ -DPO achieves an MFT of 74.29%, an MFN of 74.00%, and an MAA of 75.78%. The BWT is -0.37%, further confirming the ability for ϕ -DPO in forgetting mitigation across incremental domain adaptation. Compared to prior methods that rely on LoRA (e.g., MR-LoRA) or Mixture-of-Expert architectures (e.g., CL-MoE), ϕ -DPO offers a more unified framework while gaining superior results. These findings reinforce the generalizability and stability of ϕ -DPO in continual domain-incremental learning.

Results on the MLLM-CL Ability Benchmark. Table 2 shows results on the MLLM-CL Ability benchmark across four incremental tasks: OCR, Math & Logic (M&L), Visual Programming (VP), and GUI Agent (GUI), with the first four columns reporting performance after the final task. Our ϕ -DPO achieves consistently strong results across all tasks, with 38.40% on OCR, 39.20% on M&L, 68.65% on VP, and 35.00% on GUI Agent. In addition, ϕ -DPO outperforms prior methods on all continual learning metrics. ϕ -DPO achieves a MFT of 45.55%, MFN of 45.31%, and MAA of 43.03, while gaining a BWT of -0.31%, indicating minimal forgetting. Compared to DISCO and MR-LoRA, which rely on LoRA and routing strategies, ϕ -DPO demonstrates improved overall performance. These results highlight the

Table 2. Results on MLLM-CL Ability (* denote the method using relay data). M&L: Math and Logic, VP: Visual Perception.

Method	OCR	M&L	VP	GUI	MFT↑	MFN↑	MAA↑	BWT↑
Zeroshot [36]	31.20	30.20	60.79	10.00	33.05	—	—	—
LoRA-FT* [36]	21.80	32.70	58.38	28.75	40.32	35.41	36.32	-6.55
O-LoRA* [99]	29.60	31.30	60.79	27.50	39.96	37.30	36.34	-3.55
MoELoRA* [13]	19.80	32.20	54.19	30.00	40.35	34.05	35.39	-8.41
CL-MoE* [37]	25.40	31.80	60.91	30.00	41.22	37.03	37.28	-5.59
HiDe* [26]	24.60	28.40	30.71	23.75	36.84	26.86	33.54	-13.30
SEFE* [15]	25.60	34.80	57.61	31.39	42.25	37.35	37.93	-6.53
DISCO* [37]	34.20	35.00	61.55	27.50	40.14	39.56	37.85	-0.77
LoRA-FT [36]	23.60	33.70	55.84	32.50	41.28	36.41	36.58	-6.49
O-LoRA [99]	29.60	32.90	52.41	33.75	39.72	37.16	35.42	-3.41
MoELoRA [13]	26.70	32.80	56.85	27.22	39.45	35.89	36.07	-4.75
CL-MoE [37]	19.90	32.70	53.43	30.69	40.50	34.18	35.65	-8.43
HiDe [26]	24.60	32.10	46.32	28.75	37.98	32.94	34.60	-6.72
SEFE [15]	26.00	33.40	57.74	33.75	40.98	37.72	36.59	-4.35
DISCO [27]	32.90	33.10	60.15	30.14	39.02	39.07	36.57	0.07
MR-LoRA [116]	33.70	36.20	65.10	32.50	41.89	41.88	38.86	-0.02
ϕ -DPO	38.40	39.20	68.65	35.00	45.55	45.31	43.03	-0.31

effectiveness of ϕ -DPO in maintaining stability and generalization throughout the incremental learning process.

Results on the CoIN Benchmark. Table 3 shows results on the CoIN benchmark. MFT and BWT are omitted for prior methods since intermediate models were not published. The first eight columns report final-task accuracy on: ScienceQA (SciQA), ImageNet (Image), VizWiz (Viz), Grounding (Ground), TextVQA (Text), GQA, VQAv2 (VQA), and OCR. Our ϕ -DPO consistently outperforms all prior methods across these tasks. In particular, it achieves major gains on vision-centric tasks, *i.e.*, ImageNet (95.61%), VizWiz (54.55%), and OCR (68.69%), while also obtaining strong results on language and reasoning benchmarks, *i.e.*, ScienceQA (77.84%), GQA (64.32%), and VQAv2 (69.99%). Importantly, our approach maintains a high Mean Final Accuracy (MFN) of 68.86%, reflecting superior knowledge preservation across incremental tasks. ϕ -DPO further achieves the best MAA of 74.94%, demonstrating stable performance throughout continual training. These results confirm the effectiveness of ϕ -DPO in mitigating catastrophic forgetting and increasing adaptability.

4.3. Ablation Study

Effectiveness of Fairness DPO. Table 4 presents an ablation study on the impact of each component in our approach. Compared to knowledge distillation (KD), vanilla DPO achieves consistently better performance across in-

Table 3. Results on CoIN. SciQA: ScienceQA, Image: ImageNet, Viz: VizWiz, Ground: Grounding, Text: TextVQA, VQA: VQAv2.

Method	SciQA	Image	Viz	Ground	Text	GQA	VQA	OCR	MFN↑	MAA↑
Zeroshot	69.79	9.93	45.50	58.47	57.75	60.77	66.50	64.93	—	—
FineTune	57.43	28.90	41.88	30.05	51.39	50.76	53.28	64.78	47.31	52.86
LwF [59]	60.71	30.58	41.49	36.01	52.80	47.07	53.43	65.12	48.40	53.22
EWC [47]	59.75	31.88	42.26	34.96	51.06	51.84	55.30	64.55	48.95	53.30
L2P [101]	70.21	23.31	44.21	43.76	56.25	58.46	62.32	64.11	52.83	53.96
O-LoRA [99]	72.56	62.84	48.43	58.97	57.66	59.14	63.21	63.31	60.77	62.30
MoELoRA [13]	62.02	37.21	43.32	33.22	52.05	53.12	57.92	65.75	50.58	55.24
HiDe [26]	73.20	69.28	50.76	59.18	56.92	61.33	67.12	64.76	62.82	64.70
ϕ -DPO	77.84	95.61	54.55	60.74	59.17	64.32	69.99	68.69	68.86	74.94

Table 4. Effectiveness of Our Fairness DPO.

	RS	Med	AD	Sci	Fin	MFT↑	MFN↑	MAA↑	BWT↑
Zeroshot	32.29	28.28	15.59	35.55	62.56	34.85	—	—	—
LoRA-FT	69.65	41.59	25.43	40.88	87.45	64.98	53.00	61.13	-14.97
KD	77.82	63.92	52.88	58.57	92.85	71.37	69.21	71.49	-2.71
DPO	82.26	67.12	55.79	59.58	93.94	72.80	71.74	73.68	-1.33
ϕ -DPO	85.68	69.74	57.73	61.55	95.28	74.29	74.00	75.68	-0.37

cremental domains, *i.e.* RS (82.26%), Med (67.12%), AD (55.79%), Sci (59.58%), and Fin (93.94%), as well as improved continual learning metrics: MFT of 72.80%, MFN of 71.74%, MAA of 73.68%, and BWT of -1.33%, indicating reduced forgetting. Our ϕ -DPO further improves the performance, *i.e.* 74.29% MFT, 74.00% MFN, 75.68% MAA, and -0.37% BWT, demonstrating stronger task performance and greater stability. These results highlight the effectiveness of our Fair DPO loss in continual learning.

Effectiveness of Divergence Parameter β . Table 5 studies the impact of the divergence parameter β in our approach. The β parameter controls the trade-off between adaptability to new tasks and the forgetting level of previous knowledge. As shown in Table 5, lower values of β (*i.e.*, 0.01 and 0.05) lead to faster adaptation, reflected in higher MFT scores (75.43% and 75.27%). However, it will result in increased forgetting, as indicated by degraded BWT values (-2.66% and -1.66%). Meanwhile, larger values of β (*i.e.*, 0.50) reduce forgetting with improved BWT (-0.32%), but at the cost of reduced overall performance, including lower MFT (72.11%), MFN (71.85%), and MAA (73.60%). Among our configurations, $\beta = 0.10$ achieves the best balance, with competitive MFT (74.29%), MFN (74.00%), and MAA (75.68%), while maintaining a favorable BWT of -0.37%. These results have illustrated the role of β in stability and plasticity in continual learning.

Effectiveness of Focusing Parameter γ . Table 6 presents an ablation on the focusing parameter γ , which controls the emphasis on harder preference pairs during training. When $\gamma = 0.0$, the loss reduces to the standard DPO formulation, corresponding to the vanilla DPO baseline in Table 4. Lower values of γ (*i.e.*, 0.50 and 1.00) yield moderate improvements in stability and forgetting, as reflected in reduced BWT (-1.07% and -0.77%) while maintaining competitive MFT (72.79% and 73.38%) and MAA (73.87% and 74.66%). This result suggests that incorporating moderate focus on harder examples enhances knowledge preservation without compromising adaptability. Meanwhile, the high values of γ (*e.g.*, 5.00) lead to degraded performance across most metrics, with reduced MFT (73.21%), MFN (72.18%), and MAA (74.27%), indicating that overemphasizing diffi-

Table 5. Effectiveness of Divergence Parameter β .

β	RS	Med	AD	Sci	Fin	MFT↑	MFN↑	MAA↑	BWT↑
0.01	83.09	67.71	56.90	62.06	96.77	75.43	73.31	75.83	-2.66
0.05	84.91	69.30	57.16	62.21	96.12	75.27	73.94	76.27	-1.66
0.10	85.68	69.74	57.73	61.55	95.28	74.29	74.00	75.68	-0.37
0.50	83.74	67.55	55.44	59.64	92.88	72.11	71.85	73.60	-0.32

Table 6. Effectiveness of Focusing Parameter γ .

γ	RS	Med	AD	Sci	Fin	MFT↑	MFN↑	MAA↑	BWT↑
0.00	82.26	67.12	55.79	59.58	93.94	72.80	71.74	73.68	-1.33
0.50	82.84	67.84	55.50	59.71	93.78	72.79	71.93	73.87	-1.07
1.00	84.01	68.44	56.56	60.74	94.06	73.38	72.76	74.66	-0.77
2.00	85.68	69.74	57.73	61.55	95.28	74.29	74.00	75.68	-0.37
5.00	83.08	67.74	55.99	60.05	94.03	73.21	72.18	74.27	-1.29

cult pairs can lower overall learning dynamics. In our experiments, $\gamma = 2.00$ provides the best trade-off, achieving favorable MFT (74.29%), MFN (74.00%), MAA (75.68%), and BWT (-0.37%). These results have indicated the importance of focusing parameter γ in balancing plasticity and stability in our ϕ -DPO approach.

Effectiveness of Different LMMs. Table 7 evaluates ϕ -DPO across different LMMs: LLaVA-7B, LLaVA-13B, and InternVL-7B [16]. In all cases, ϕ -DPO outperforms standard DPO, confirming the generality of our Fair DPO objective. Larger models (*i.e.* LLaVA-13B) show improved performance over LLaVA-7B in MFT (76.29% vs. 74.29%), MFN (75.81% vs. 74.00%), MAA (77.57% vs. 75.68%), and BWT (-0.59% vs. -0.37%), reflecting better knowledge preservation due to greater capacity. InternVL-7B, despite similar size to LLaVA-7B, benefits from stronger vision-language alignment and achieves competitive results. ϕ -DPO consistently enhances performance across all backbones, demonstrating robustness and compatibility with diverse LMM architectures.

5. Conclusions and Limitations

Conclusions. This paper has presented a novel Fairness DPO approach to Continual Learning in LMMs. In particular, our Fair DPO learning objective has been introduced to address both catastrophic forgetting and fairness problems. Our theoretical analysis has also shown the effectiveness of our proposed approach. Our SoTA results on three benchmarks have further confirmed the effectiveness of our ϕ -DPO compared to prior methods.

Limitations. Our work adopts a set of learning hyperparameters aligned with theoretical analysis, but this choice introduces limitations, particularly in tuning β , γ , the weighted loss in Eqn. (17), and DPO data construction. The quality of DPO data is sensitive to label stability, which may be affected by class imbalance, domain shifts, or model uncertainty, potentially leading to suboptimal distillation targets and misleading pairwise correlations. These limitations highlight the need for future work on more robust and adaptive DPO strategies for continual multimodal learning.

Table 7. Effectiveness of Different LMM Framework.

LLM	Method	RS	Med	AD	Sci	Fin	MFT↑	MFN↑	MAA↑	BWT↑
LLaVA-7B	DPO	82.26	67.12	55.79	59.58	93.94	72.80	71.74	73.68	-1.33
	ϕ -DPO	85.68	69.74	57.73	61.55	95.28	74.29	74.00	75.68	-0.37
LLaVA-13B	DPO	86.24	70.28	58.02	63.26	96.84	75.89	74.93	77.00	-1.21
	ϕ -DPO	87.40	71.09	59.34	63.96	97.28	76.29	75.81	77.57	-0.59
InternVL-7B	DPO	82.69	67.69	55.97	60.67	94.83	73.88	72.37	74.68	-1.89
	ϕ -DPO	85.64	69.88	57.94	61.95	95.74	74.62	74.23	75.94	-0.49

Acknowledgment. This work is partly supported by NSF CAREER (No. 2442295), NSF SCH (No. 2501021), NSF E-RISE (No. 2445877), NSF BIO (No. 2524623) and USDA/NIFA Award. We also acknowledge the Arkansas High-Performance Computing Center (HPC) for GPU servers.

References

- [1] Manoj Acharya, Kushal Kafle, and Christopher Kanan. Tal-lyqa: Answering complex counting questions. In *Proceedings of the AAAI conference on artificial intelligence*, pages 8076–8084, 2019. 6
- [2] Josh Achiam, Steven Adler, Sandhini Agarwal, Lama Ahmad, Ilge Akkaya, Florencia Leoni Aleman, Diogo Almeida, Janko Altenschmidt, Sam Altman, Shyamal Anadkat, et al. Gpt-4 technical report. *arXiv preprint arXiv:2303.08774*, 2023. 3
- [3] Gustavo Aguilar, Yuan Ling, Yu Zhang, Benjamin Yao, Xing Fan, and Chenlei Guo. Knowledge distillation from internal representations. In *Proceedings of the AAAI conference on artificial intelligence*, pages 7350–7357, 2020. 2
- [4] Jean-Baptiste Alayrac, Jeff Donahue, Pauline Luc, Antoine Miech, Iain Barr, Yana Hasson, Karel Lenc, Arthur Mensch, Katherine Millican, Malcolm Reynolds, et al. Flamingo: a visual language model for few-shot learning. *Advances in neural information processing systems*, 35: 23716–23736, 2022. 3
- [5] Jinze Bai, Shuai Bai, Yunfei Chu, Zeyu Cui, Kai Dang, Xiaodong Deng, Yang Fan, Wenbin Ge, Yu Han, Fei Huang, et al. Qwen technical report. *arXiv preprint arXiv:2309.16609*, 2023. 1, 3
- [6] Jinze Bai, Shuai Bai, Shusheng Yang, Shijie Wang, Sinan Tan, Peng Wang, Junyang Lin, Chang Zhou, and Jingren Zhou. Qwen-vl: A versatile vision-language model for understanding, localization, text reading, and beyond. *arXiv preprint arXiv:2308.12966*, 1(2):3, 2023. 3
- [7] Pietro Buzzega, Matteo Boschini, Angelo Porrello, Davide Abati, and Simone Calderara. Dark experience for general continual learning: a strong, simple baseline. *Advances in neural information processing systems*, 33:15920–15930, 2020. 3
- [8] Meng Cao, Yuyang Liu, Yingfei Liu, Tiancai Wang, Jiahua Dong, Henghui Ding, Xiangyu Zhang, Ian Reid, and Xiaodan Liang. Continual llava: Continual instruction tuning in large vision-language models. *arXiv preprint arXiv:2411.02564*, 2024. 3
- [9] Patrick Cattiaux and Arnaud Guillin. A criterion for tagrand’s quadratic transportation cost inequality. *arXiv preprint math/0312081*, 2003. 15
- [10] Fabio Cermelli, Massimiliano Mancini, Samuel Rota Bulò, Elisa Ricci, and Barbara Caputo. Modeling the background for incremental learning in semantic segmentation. In *CVPR*, 2020. 2, 3, 4, 5
- [11] Shuaichen Chang, David Palzer, Jialin Li, Eric Fosler-Lussier, and Ningchuan Xiao. Mapqa: A dataset for question answering on choropleth maps. *arXiv preprint arXiv:2211.08545*, 2022. 6
- [12] Yupeng Chang, Yi Chang, and Yuan Wu. Ba-lora: Bias-alleviating low-rank adaptation to mitigate catastrophic inheritance in large language models, 2025. 2
- [13] Cheng Chen, Junchen Zhu, Xu Luo, Heng T Shen, Jingkuan Song, and Lianli Gao. Coin: A benchmark of continual instruction tuning for multimodal large language models. *Advances in Neural Information Processing Systems*, 37: 57817–57840, 2024. 2, 3, 6, 7
- [14] Jiayi Chen and Aidong Zhang. FedMBSBridge: Bridgeable multimodal federated learning. In *Forty-first International Conference on Machine Learning*, 2024. 3
- [15] Jinpeng Chen, Runmin Cong, Yuzhi Zhao, Hongzheng Yang, Guangneng Hu, Horace Ho Shing Ip, and Sam Kwong. Sefe: Superficial and essential forgetting eliminator for multimodal continual instruction tuning. *arXiv preprint arXiv:2505.02486*, 2025. 3, 7
- [16] Zhe Chen, Jiannan Wu, Wenhai Wang, Weijie Su, Guo Chen, Sen Xing, Muyan Zhong, Qinglong Zhang, Xizhou Zhu, Lewei Lu, et al. Internvl: Scaling up vision foundation models and aligning for generic visual-linguistic tasks. In *Proceedings of the IEEE/CVF conference on computer vision and pattern recognition*, pages 24185–24198, 2024. 8
- [17] Wei-Lin Chiang, Zhuohan Li, Zi Lin, Ying Sheng, Zhanghao Wu, Hao Zhang, Lianmin Zheng, Siyuan Zhuang, Yonghao Zhuang, Joseph E. Gonzalez, Ion Stoica, and Eric P. Xing. Vicuna: An open-source chatbot impressing gpt-4 with 90%* chatgpt quality, 2023. 3, 6
- [18] Andrea Cossu, Antonio Carta, Lucia Passaro, Vincenzo Lomonaco, Tinne Tuytelaars, and Davide Bacciu. Continual pre-training mitigates forgetting in language and vision. *Neural Networks*, 179:106492, 2024. 3
- [19] Matt Deitke, Christopher Clark, Sangho Lee, Rohun Tripathi, Yue Yang, Jae Sung Park, Mohammadreza Salehi, Niklas Muennighoff, Kyle Lo, Luca Soldaini, et al. Molmo and pixmo: Open weights and open data for state-of-the-art vision-language models. In *Proceedings of the Computer Vision and Pattern Recognition Conference*, pages 91–104, 2025. 1
- [20] Jia Deng, Wei Dong, Richard Socher, Li-Jia Li, Kai Li, and Li Fei-Fei. Imagenet: A large-scale hierarchical image database. In *2009 IEEE conference on computer vision and pattern recognition*, pages 248–255. Ieee, 2009. 6
- [21] Arthur Douillard, Yifu Chen, Arnaud Dapogny, and Matthieu Cord. Plop: Learning without forgetting for continual semantic segmentation. In *Proceedings of the IEEE/CVF Conference on Computer Vision and Pattern Recognition*, pages 4040–4050, 2021. 2, 3, 4, 5
- [22] Arthur Douillard, Alexandre Ramé, Guillaume Couairon, and Matthieu Cord. Dyttox: Transformers for continual learning with dynamic token expansion. In *Proceedings of the IEEE/CVF conference on computer vision and pattern recognition*, pages 9285–9295, 2022. 3
- [23] David A Edwards. On the kantorovich–rubinstein theorem. *Expositiones Mathematicae*, 29(4):387–398, 2011. 14

- [24] Deepanway Ghosal, Navonil Majumder, Ambuj Mehrish, and Soujanya Poria. Text-to-audio generation using instruction-tuned llm and latent diffusion model. *arXiv preprint arXiv:2304.13731*, 2023. 3
- [25] Yash Goyal, Tejas Khot, Douglas Summers-Stay, Dhruv Batra, and Devi Parikh. Making the v in vqa matter: Elevating the role of image understanding in visual question answering. In *Proceedings of the IEEE conference on computer vision and pattern recognition*, pages 6904–6913, 2017. 6
- [26] Haiyang Guo, Fanhu Zeng, Ziwei Xiang, Fei Zhu, Da-Han Wang, Xu-Yao Zhang, and Cheng-Lin Liu. Hidelava: Hierarchical decoupling for continual instruction tuning of multimodal large language model. *arXiv preprint arXiv:2503.12941*, 2025. 2, 3, 6, 7
- [27] Haiyang Guo, Fanhu Zeng, Fei Zhu, Wenzhuo Liu, Da-Han Wang, Jian Xu, Xu-Yao Zhang, and Cheng-Lin Liu. Federated continual instruction tuning. *arXiv preprint arXiv:2503.12897*, 2025. 7
- [28] Haiyang Guo, Fanhu Zeng, Fei Zhu, Jiayi Wang, Xukai Wang, Jingang Zhou, Hongbo Zhao, Wenzhuo Liu, Shijie Ma, Xu-Yao Zhang, et al. A comprehensive survey on continual learning in generative models. *arXiv preprint arXiv:2506.13045*, 2025. 3
- [29] Ziyu Guo, Ray Zhang, Hao Chen, Jialin Gao, Dongzhi Jiang, Jiaze Wang, and Pheng-Ann Heng. Sciverse: Unveiling the knowledge comprehension and visual reasoning of llms on multi-modal scientific problems. *arXiv preprint arXiv:2503.10627*, 2025. 6
- [30] Danna Gurari, Qing Li, Abigale J Stangl, Anhong Guo, Chi Lin, Kristen Grauman, Jiebo Luo, and Jeffrey P Bigham. Vizwiz grand challenge: Answering visual questions from blind people. In *Proceedings of the IEEE conference on computer vision and pattern recognition*, pages 3608–3617, 2018. 6
- [31] Jiayi Han, Liang Du, Hongwei Du, Xiangguo Zhou, Yiwen Wu, Weibo Zheng, and Donghong Han. Slim: Let llm learn more and forget less with soft lora and identity mixture. *arXiv preprint arXiv:2410.07739*, 2024. 2
- [32] Ryo Hase, Md Rafi Ur Rashid, Ashley Lewis, Jing Liu, Toshiaki Koike-Akino, Kieran Parsons, and Ye Wang. Smoothed embeddings for robust language models. *arXiv preprint arXiv:2501.16497*, 2025. 14
- [33] Xuehai He, Yichen Zhang, Luntian Mou, Eric Xing, and Pengtao Xie. Pathvqa: 30000+ questions for medical visual question answering. *arXiv preprint arXiv:2003.10286*, 2020. 6
- [34] Calypso Herrera, Florian Krach, and Josef Teichmann. Local lipschitz bounds of deep neural networks. *arXiv preprint arXiv:2004.13135*, 2020. 14
- [35] Yu-Chung Hsiao, Fedir Zubach, Gilles Baechler, Victor Carbune, Jason Lin, Maria Wang, Srinivas Sunkara, Yun Zhu, and Jindong Chen. Screenqa: Large-scale question-answer pairs over mobile app screenshots. *arXiv preprint arXiv:2209.08199*, 2022. 6
- [36] Edward J Hu, Yelong Shen, Phillip Wallis, Zeyuan Allen-Zhu, Yuanzhi Li, Shean Wang, Lu Wang, Weizhu Chen, et al. Lora: Low-rank adaptation of large language models. *ICLR*, 1(2):3, 2022. 2, 7
- [37] Tianyu Huai, Jie Zhou, Xingjiao Wu, Qin Chen, Qingchun Bai, Ze Zhou, and Liang He. Cl-moe: Enhancing multimodal large language model with dual momentum mixture-of-experts for continual visual question answering. In *Proceedings of the Computer Vision and Pattern Recognition Conference*, pages 19608–19617, 2025. 7
- [38] Drew A Hudson and Christopher D Manning. Gqa: A new dataset for real-world visual reasoning and compositional question answering. In *Proceedings of the IEEE/CVF conference on computer vision and pattern recognition*, pages 6700–6709, 2019. 6
- [39] Atin Sakkeer Hussain, Shansong Liu, Chenshuo Sun, and Ying Shan. M2ugen: Multi-modal music understanding and generation with the power of large language models. *arXiv preprint arXiv:2311.11255*, 2023. 3
- [40] Goeric Huybrechts, Srikanth Ronanki, Sai Muralidhar Jayanthi, Jack Fitzgerald, and Srinivasan Veeravanallur. Document haystack: A long context multimodal image/document understanding vision llm benchmark. *arXiv preprint arXiv:2507.15882*, 2025. 1
- [41] Amit Kumar Jaiswal, Haiming Liu, and Ingo Frommholz. Multimodal rag enhanced visual description. *arXiv preprint arXiv:2508.09170*, 2025. 1
- [42] Joel Jang, Seonghyeon Ye, Changho Lee, Sohee Yang, Joongbo Shin, Janghoon Han, Gyeonghun Kim, and Minjoon Seo. Temporalwiki: A lifelong benchmark for training and evaluating ever-evolving language models. *arXiv preprint arXiv:2204.14211*, 2022. 3
- [43] Justin Johnson, Bharath Hariharan, Laurens Van Der Maaten, Li Fei-Fei, C Lawrence Zitnick, and Ross Girshick. Clevr: A diagnostic dataset for compositional language and elementary visual reasoning. In *Proceedings of the IEEE conference on computer vision and pattern recognition*, pages 2901–2910, 2017. 6
- [44] Sahar Kazemzadeh, Vicente Ordonez, Mark Matten, and Tamara Berg. Referitgame: Referring to objects in photographs of natural scenes. In *Proceedings of the 2014 conference on empirical methods in natural language processing (EMNLP)*, pages 787–798, 2014. 6
- [45] Aniruddha Kembhavi, Mike Salvato, Eric Kolve, Minjoon Seo, Hannaneh Hajishirzi, and Ali Farhadi. A diagram is worth a dozen images, 2016. 6
- [46] Aniruddha Kembhavi, Minjoon Seo, Dustin Schwenk, Jonghyun Choi, Ali Farhadi, and Hannaneh Hajishirzi. Are you smarter than a sixth grader? textbook question answering for multimodal machine comprehension. In *Proceedings of the IEEE Conference on Computer Vision and Pattern Recognition*, pages 4999–5007, 2017. 6
- [47] James Kirkpatrick, Razvan Pascanu, Neil Rabinowitz, Joel Veness, Guillaume Desjardins, Andrei A Rusu, Kieran Milan, John Quan, Tiago Ramalho, Agnieszka Grabska-Barwinska, et al. Overcoming catastrophic forgetting in neural networks. *Proceedings of the national academy of sciences*, 114(13):3521–3526, 2017. 3, 7
- [48] Frantzeska Lavda, Jason Ramapuram, Magda Gregorova, and Alexandros Kalousis. Continual classification learning

- using generative models. *arXiv preprint arXiv:1810.10612*, 2018. 3
- [49] Michel Ledoux, Ivan Nourdin, and Giovanni Peccati. Stein’s method, logarithmic sobolev and transport inequalities. *Geometric and Functional Analysis*, 25(1):256–306, 2015. 15
- [50] Bo Li, Hao Zhang, Kaichen Zhang, Dong Guo, Yuanhan Zhang, Renrui Zhang, Feng Li, Ziwei Liu, and Chunyuan Li. Llava-next: What else influences visual instruction tuning beyond data?, 2024. 3
- [51] Bo Li, Kaichen Zhang, Hao Zhang, Dong Guo, Renrui Zhang, Feng Li, Yuanhan Zhang, Ziwei Liu, and Chunyuan Li. Llava-next: Stronger llms supercharge multimodal capabilities in the wild, 2024. 3
- [52] Bo Li, Yuanhan Zhang, Dong Guo, Renrui Zhang, Feng Li, Hao Zhang, Kaichen Zhang, Yanwei Li, Ziwei Liu, and Chunyuan Li. Llava-onevision: Easy visual task transfer. *arXiv preprint arXiv:2408.03326*, 2024. 3
- [53] Chunyuan Li, Cliff Wong, Sheng Zhang, Naoto Usuyama, Haotian Liu, Jianwei Yang, Tristan Naumann, Hoifung Poon, and Jianfeng Gao. Llava-med: Training a large language-and-vision assistant for biomedicine in one day. *Advances in Neural Information Processing Systems*, 36, 2024. 3
- [54] Feng Li, Renrui Zhang, Hao Zhang, Yuanhan Zhang, Bo Li, Wei Li, Zejun Ma, and Chunyuan Li. Llava-next: Tackling multi-image, video, and 3d in large multimodal models, 2024. 3
- [55] Junnan Li, Dongxu Li, Caiming Xiong, and Steven Hoi. Blip: Bootstrapping language-image pre-training for unified vision-language understanding and generation. In *International Conference on Machine Learning*, pages 12888–12900. PMLR, 2022. 1
- [56] Junnan Li, Dongxu Li, Silvio Savarese, and Steven Hoi. Blip-2: Bootstrapping language-image pre-training with frozen image encoders and large language models. In *International conference on machine learning*, pages 19730–19742. PMLR, 2023. 1, 3
- [57] KunChang Li, Yanan He, Yi Wang, Yizhuo Li, Wenhai Wang, Ping Luo, Yali Wang, Limin Wang, and Yu Qiao. Videochat: Chat-centric video understanding. *arXiv preprint arXiv:2305.06355*, 2023. 3
- [58] Yanwei Li, Chengyao Wang, and Jiaya Jia. Llama-vid: An image is worth 2 tokens in large language models. In *European Conference on Computer Vision*, pages 323–340. Springer, 2025. 3
- [59] Zhizhong Li and Derek Hoiem. Learning without forgetting. *IEEE transactions on pattern analysis and machine intelligence*, 40(12):2935–2947, 2017. 3, 7
- [60] Zhang Li, Biao Yang, Qiang Liu, Zhiyin Ma, Shuo Zhang, Jingxu Yang, Yabo Sun, Yuliang Liu, and Xiang Bai. Monkey: Image resolution and text label are important things for large multi-modal models. In *proceedings of the IEEE/CVF conference on computer vision and pattern recognition*, pages 26763–26773, 2024. 6
- [61] Bin Lin, Yang Ye, Bin Zhu, Jiayi Cui, Munan Ning, Peng Jin, and Li Yuan. Video-llava: Learning united visual representation by alignment before projection. *arXiv preprint arXiv:2311.10122*, 2023. 3
- [62] Jessy Lin, Luke Zettlemoyer, Gargi Ghosh, Wen-Tau Yih, Aram Markosyan, Vincent-Pierre Berges, and Barlas Oğuz. Continual learning via sparse memory finetuning. *arXiv preprint arXiv:2510.15103*, 2025. 3
- [63] Tsung-Yi Lin, Priya Goyal, Ross Girshick, Kaiming He, and Piotr Dollár. Focal loss for dense object detection. In *Proceedings of the IEEE international conference on computer vision*, pages 2980–2988, 2017. 5
- [64] Dingning Liu, Xiaoshui Huang, Yuenan Hou, Zhihui Wang, Zhen fei Yin, Yongshun Gong, Peng Gao, and Wanli Ouyang. Uni3d-llm: Unifying point cloud perception, generation and editing with large language models. *ArXiv*, abs/2402.03327, 2024. 3
- [65] Haotian Liu, Chunyuan Li, Yuheng Li, and Yong Jae Lee. Improved baselines with visual instruction tuning. In *Proceedings of the IEEE/CVF Conference on Computer Vision and Pattern Recognition*, pages 26296–26306, 2024. 1, 3, 6
- [66] Haotian Liu, Chunyuan Li, Yuheng Li, Bo Li, Yuanhan Zhang, Sheng Shen, and Yong Jae Lee. Llava-next: Improved reasoning, ocr, and world knowledge, 2024. 3
- [67] Haotian Liu, Chunyuan Li, Qingyang Wu, and Yong Jae Lee. Visual instruction tuning. *Advances in neural information processing systems*, 36, 2024. 1, 3
- [68] Yuliang Liu, Zhang Li, Mingxin Huang, Biao Yang, Wenwen Yu, Chunyuan Li, Xu-Cheng Yin, Cheng-Lin Liu, Lianwen Jin, and Xiang Bai. Ocrbench: on the hidden mystery of ocr in large multimodal models. *Science China Information Sciences*, 67(12):220102, 2024. 6
- [69] Sylvain Lobry, Diego Marcos, Jesse Murray, and Devis Tuia. Rsvqa: Visual question answering for remote sensing data. *IEEE Transactions on Geoscience and Remote Sensing*, 58(12):8555–8566, 2020. 6
- [70] Pan Lu, Swaroop Mishra, Tanglin Xia, Liang Qiu, Kai-Wei Chang, Song-Chun Zhu, Oyvind Tafjord, Peter Clark, and Ashwin Kalyan. Learn to explain: Multimodal reasoning via thought chains for science question answering. *Advances in Neural Information Processing Systems*, 35: 2507–2521, 2022. 6
- [71] Arun Mallya, Dillon Davis, and Svetlana Lazebnik. Piggyback: Adapting a single network to multiple tasks by learning to mask weights. In *Proceedings of the European conference on computer vision (ECCV)*, pages 67–82, 2018. 3
- [72] Junhua Mao, Jonathan Huang, Alexander Toshev, Oana Camburu, Alan L Yuille, and Kevin Murphy. Generation and comprehension of unambiguous object descriptions. In *Proceedings of the IEEE conference on computer vision and pattern recognition*, pages 11–20, 2016. 6
- [73] Anand Mishra, Shashank Shekhar, Ajeet Kumar Singh, and Anirban Chakraborty. Ocr-vqa: Visual question answering by reading text in images. In *2019 international conference on document analysis and recognition (ICDAR)*, pages 947–952. IEEE, 2019. 6
- [74] Yiqiao Qiu, Yixing Shen, Zhuohao Sun, Yanchong Zheng, Xiaobin Chang, Weishi Zheng, and Ruixuan Wang. Sats:

- Self-attention transfer for continual semantic segmentation. *Pattern Recognition*, 138:109383, 2023. 2
- [75] Rafael Rafailov, Archit Sharma, Eric Mitchell, Christopher D Manning, Stefano Ermon, and Chelsea Finn. Direct preference optimization: Your language model is secretly a reward model. *Advances in neural information processing systems*, 36:53728–53741, 2023. 4
- [76] Anastasia Razdaibiedina, Yuning Mao, Rui Hou, Madian Khabsa, Mike Lewis, and Amjad Almahairi. Progressive prompts: Continual learning for language models. *arXiv preprint arXiv:2301.12314*, 2023. 3
- [77] John Schulman, Filip Wolski, Prafulla Dhariwal, Alec Radford, and Oleg Klimov. Proximal policy optimization algorithms. *arXiv preprint arXiv:1707.06347*, 2017. 4
- [78] Wei Shen, Jiangbo Pei, Yi Peng, Xuchen Song, Yang Liu, Jian Peng, Haofeng Sun, Yunzhuo Hao, Peiyu Wang, Jianhao Zhang, and Yahui Zhou. Skywork-r1v3 technical report, 2025. 3
- [79] Haizhou Shi, Zihao Xu, Hengyi Wang, Weiyi Qin, Wenyuan Wang, Yibin Wang, Zifeng Wang, Sayna Ebrahimi, and Hao Wang. Continual learning of large language models: A comprehensive survey. *ACM Computing Surveys*, 2024. 3
- [80] Wenhao Shi, Zhiqiang Hu, Yi Bin, Junhua Liu, Yang Yang, See-Kiong Ng, Lidong Bing, and Roy Ka-Wei Lee. Math-llava: Bootstrapping mathematical reasoning for multimodal large language models. *arXiv preprint arXiv:2406.17294*, 2024. 6
- [81] Zenglin Shi, Pei Liu, Tong Su, Yunpeng Wu, Kuiren Liu, Yu Song, and Meng Wang. Densely distilling cumulative knowledge for continual learning. *arXiv preprint arXiv:2405.09820*, 2024. 2
- [82] Marco Siino. Mcrock at semeval-2024 task 4: Mistral 7b for multilingual detection of persuasion techniques in memes. In *Proceedings of the 18th International Workshop on Semantic Evaluation (SemEval-2024)*, pages 53–59, 2024. 3
- [83] Chonghao Sima, Katrin Renz, Kashyap Chitta, Li Chen, Hanxue Zhang, Chengen Xie, Jens Beißwenger, Ping Luo, Andreas Geiger, and Hongyang Li. Drivelm: Driving with graph visual question answering. In *European conference on computer vision*, pages 256–274. Springer, 2024. 6
- [84] Amanpreet Singh, Vivek Natarajan, Meet Shah, Yu Jiang, Xinlei Chen, Dhruv Batra, Devi Parikh, and Marcus Rohrbach. Towards vqa models that can read. In *Proceedings of the IEEE/CVF conference on computer vision and pattern recognition*, pages 8317–8326, 2019. 6
- [85] James Seale Smith, Leonid Karlinsky, Vyshnavi Gutta, Paola Cascante-Bonilla, Donghyun Kim, Assaf Arbelle, Rameswar Panda, Rogerio Feris, and Zsolt Kira. Coda-prompt: Continual decomposed attention-based prompting for rehearsal-free continual learning. In *Proceedings of the IEEE/CVF conference on computer vision and pattern recognition*, pages 11909–11919, 2023. 3
- [86] Alane Suhr and Yoav Artzi. Continual learning for instruction following from realtime feedback. *Advances in Neural Information Processing Systems*, 36:32340–32359, 2023. 3
- [87] Ryota Tanaka, Taichi Iki, Taku Hasegawa, Kyosuke Nishida, Kuniko Saito, and Jun Suzuki. Vdocrag: Retrieval-augmented generation over visually-rich documents. In *Proceedings of the Computer Vision and Pattern Recognition Conference*, pages 24827–24837, 2025. 1
- [88] Yonglong Tian, Dilip Krishnan, and Phillip Isola. Contrastive representation distillation. *arXiv preprint arXiv:1910.10699*, 2019. 2
- [89] Thanh-Dat Truong, Chi Nhan Duong, Ngan Le, Son Lam Phung, Chase Rainwater, and Khoa Luu. Bimal: Bijective maximum likelihood approach to domain adaptation in semantic scene segmentation. In *Proceedings of the IEEE/CVF International Conference on Computer Vision*, pages 8548–8557, 2021. 3
- [90] Thanh-Dat Truong, Ngan Le, Bhiksha Raj, Jackson Cothren, and Khoa Luu. Freedom: Fairness domain adaptation approach to semantic scene understanding. In *IEEE/CVF Computer Vision and Pattern Recognition (CVPR)*, 2023. 3
- [91] Thanh-Dat Truong, Hoang-Quan Nguyen, Bhiksha Raj, and Khoa Luu. Fairness continual learning approach to semantic scene understanding in open-world environments. *Advances in Neural Information Processing Systems*, 36: 65456–65467, 2023. 2, 3
- [92] Thanh-Dat Truong, Hoang-Quan Nguyen, Bhiksha Raj, and Khoa Luu. Fairness continual learning approach to semantic scene understanding in open-world environments. *Advances in Neural Information Processing Systems*, 36, 2024. 3
- [93] Thanh-Dat Truong, Utsav Prabhu, Dongyi Wang, Bhiksha Raj, Susan Gauch, Jeyamkondan Subbiah, and Khoa Luu. Eagle: Efficient adaptive geometry-based learning in cross-view understanding. *Advances in Neural Information Processing Systems*, 37:137309–137333, 2024. 3
- [94] Thanh-Dat Truong, Utsav Prabhu, Bhiksha Raj, Jackson Cothren, and Khoa Luu. Falcon: Fairness learning via contrastive attention approach to continual semantic scene understanding. In *Proceedings of the Computer Vision and Pattern Recognition Conference*, pages 15065–15075, 2025. 2, 3
- [95] Thanh-Dat Truong, Huu-Thien Tran, Tran Thai Son, Bhiksha Raj, and Khoa Luu. Directed-tokens: A robust multimodality alignment approach to large language-vision models. In *The Thirty-ninth Annual Conference on Neural Information Processing Systems*, 2025. 3
- [96] Bryan Wang, Gang Li, Xin Zhou, Zhourong Chen, Tovi Grossman, and Yang Li. Screen2words: Automatic mobile ui summarization with multimodal learning. In *The 34th Annual ACM Symposium on User Interface Software and Technology*, pages 498–510, 2021. 6
- [97] Shuchan Wang, Photios A Stavrou, and Mikael Skoglund. Generalizations of talagrand inequality for sinkhorn distance using entropy power inequality. *Entropy*, 24(2):306, 2022. 15
- [98] Weiyun Wang, Zhangwei Gao, Lixin Gu, Hengjun Pu, Long Cui, Xingguang Wei, Zhaoyang Liu, Linglin Jing, Shenglong Ye, Jie Shao, et al. Internvl3.5: Advancing open-

- source multimodal models in versatility, reasoning, and efficiency, 2025. 3
- [99] Xiao Wang, Tianze Chen, Qiming Ge, Han Xia, Rong Bao, Rui Zheng, Qi Zhang, Tao Gui, and Xuanjing Huang. Orthogonal subspace learning for language model continual learning. *arXiv preprint arXiv:2310.14152*, 2023. 3, 7
- [100] Yidong Wang, Zhuohao Yu, Jindong Wang, Qiang Heng, Hao Chen, Wei Ye, Rui Xie, Xing Xie, and Shikun Zhang. Exploring vision-language models for imbalanced learning. *International Journal of Computer Vision*, 132(1):224–237, 2024. 2
- [101] Zifeng Wang, Zizhao Zhang, Chen-Yu Lee, Han Zhang, Ruoxi Sun, Xiaoqi Ren, Guolong Su, Vincent Perot, Jennifer Dy, and Tomas Pfister. Learning to prompt for continual learning. In *Proceedings of the IEEE/CVF conference on computer vision and pattern recognition*, pages 139–149, 2022. 3, 7
- [102] Yuetian Weng, Mingfei Han, Haoyu He, Xiaojun Chang, and Bohan Zhuang. Longvlm: Efficient long video understanding via large language models. *arXiv preprint arXiv:2404.03384*, 2024. 3
- [103] Runsen Xu, Xiaolong Wang, Tai Wang, Yilun Chen, Jiangmiao Pang, and Dahua Lin. Pointllm: Empowering large language models to understand point clouds. In *ECCV*, 2024. 3
- [104] Senqiao Yang, Jiaming Liu, Ray Zhang, Mingjie Pan, Zoey Guo, Xiaoqi Li, Zehui Chen, Peng Gao, Yandong Guo, and Shanghang Zhang. Lidar-llm: Exploring the potential of large language models for 3d lidar understanding. *arXiv preprint arXiv:2312.14074*, 2023. 3
- [105] Muchao Ye, Ziyi Yin, Tianrong Zhang, Tianyu Du, Jinghui Chen, Ting Wang, and Fenglong Ma. Unit: a unified look at certified robust training against text adversarial perturbation. *Advances in Neural Information Processing Systems*, 36:22351–22368, 2023. 14
- [106] Wenpeng Yin, Jia Li, and Caiming Xiong. Contintin: Continual learning from task instructions. *arXiv preprint arXiv:2203.08512*, 2022. 3
- [107] Kaining Ying, Fanqing Meng, Jin Wang, Zhiqian Li, Han Lin, Yue Yang, Hao Zhang, Wenbo Zhang, Yuqi Lin, Shuo Liu, et al. Mmt-bench: A comprehensive multimodal benchmark for evaluating large vision-language models towards multitask agi. *arXiv preprint arXiv:2404.16006*, 2024. 6
- [108] Shi Yu, Chaoyue Tang, Bokai Xu, Junbo Cui, Junhao Ran, Yukun Yan, Zhenghao Liu, Shuo Wang, Xu Han, Zhiyuan Liu, et al. Visrag: Vision-based retrieval-augmented generation on multi-modality documents. *arXiv preprint arXiv:2410.10594*, 2024. 1
- [109] Daoguang Zan, Bei Chen, Dejian Yang, Zeqi Lin, Minsu Kim, Bei Guan, Yongji Wang, Weizhu Chen, and Jian-Guang Lou. Cert: continual pre-training on sketches for library-oriented code generation. *arXiv preprint arXiv:2206.06888*, 2022. 3
- [110] Fanhu Zeng, Fei Zhu, Haiyang Guo, Xu-Yao Zhang, and Cheng-Lin Liu. Modalprompt: Towards efficient multimodal continual instruction tuning with dual-modality guided prompt. *arXiv preprint arXiv:2410.05849*, 2024. 3
- [111] Han Zhang, Yu Lei, Lin Gui, Min Yang, Yulan He, Hui Wang, and Ruifeng Xu. Cppo: Continual learning for reinforcement learning with human feedback. In *The Twelfth International Conference on Learning Representations*, 2024. 3
- [112] Rongzhi Zhang, Jiaming Shen, Tianqi Liu, Jialu Liu, Michael Bendersky, Marc Najork, and Chao Zhang. Do not blindly imitate the teacher: Using perturbed loss for knowledge distillation. *arXiv preprint arXiv:2305.05010*, 2023. 2
- [113] Renrui Zhang, Xinyu Wei, Dongzhi Jiang, Ziyu Guo, Shicheng Li, Yichi Zhang, Chengzhuo Tong, Jiaming Liu, Aojun Zhou, Bin Wei, et al. Mavis: Mathematical visual instruction tuning with an automatic data engine. *arXiv preprint arXiv:2407.08739*, 2024. 6
- [114] Xin Zhang, Liang Bai, Xian Yang, and Jiye Liang. Clora: Continual low-rank adaptation for pre-trained models. *arXiv preprint arXiv:2502.17920*, 2025. 2
- [115] Yuanhan Zhang, Bo Li, haotian Liu, Yong jae Lee, Liangke Gui, Di Fu, Jiashi Feng, Ziwei Liu, and Chunyuan Li. Llava-next: A strong zero-shot video understanding model, 2024. 3
- [116] Hongbo Zhao, Fei Zhu, Haiyang Guo, Meng Wang, Rundong Wang, Gaofeng Meng, and Zhaoxiang Zhang. Mllm-cl: Continual learning for multimodal large language models. *arXiv preprint arXiv:2506.05453*, 2025. 1, 2, 3, 6, 7
- [117] Yue Zhao, Ishan Misra, Philipp Krähenbühl, and Rohit Girdhar. Learning video representations from large language models. In *Proceedings of the IEEE/CVF Conference on Computer Vision and Pattern Recognition*, pages 6586–6597, 2023. 3

ϕ -DPO: Fairness Direct Preference Optimization Approach to Continual Learning in Large Multimodal Models Supplementary Material

A. Proof of Lemmas

A.1. Proof of Lemma 1

The DPO loss in Eqn. (7) can be rewrite as follows:

$$\begin{aligned} \mathcal{L}_{\text{DPO}}(\pi_t, \pi_{t-1}) &= \mathbb{E}_{x, y^+, y^-} \left[\ell_\beta(\Delta_t(y^+, y^-)) \right] \\ \ell_\beta(u) &= \log(1 + \exp(\beta u)) \\ \Delta_t(y^+, y^-) &= \left(\log \pi_t(y^+|x) - \log \pi_t(y^-|x) \right) \\ &\quad - \left(\log \pi_{t-1}(y^+|x) - \log \pi_{t-1}(y^-|x) \right) \end{aligned} \quad (18)$$

Lemma 4 *Pairwise Logistic Lower Bound by Margin.* For any $u \in \mathbb{R}$ and $\beta > 0$,

$$\ell_\beta(u) = \log(1 + e^{-\beta u}) \geq \log 2 - \frac{\beta}{2}u.$$

Proof. Since $\log(1 + e^{-v})$ is convex and symmetric around $v = 0$ in the sense that its tangent at 0 is $\log 2 - \frac{1}{2}v$, the global underestimator follows from convexity $\log(1 + e^{-v}) \geq \log 2 - \frac{1}{2}v$. Then, we substitute $v = \beta u$ follow by taking expectation over pairs:

$$\mathbb{E}[\ell_\beta(\Delta_t(y^+, y^-))] \geq \log 2 - \frac{\beta}{2} \mathbb{E}[\Delta_t(y^+, y^-)]. \quad (19)$$

As a result, the small value of the DPO loss forces large average margin $\mathbb{E}[\Delta_t(y^+, y^-)]$. In other words, the smaller value of DPO loss enforces the model’s preference for well-retained y^+ responses stronger than for forgotten ones y^- .

Lemma 5 *Average Margin Controls an Integral Probability Metrics (IPM).* Let \mathcal{F}_1 be the set of all 1-Lipschitz functions, If the reward function r is L -Lipschitz, then $r/L \in \mathcal{F}_1$. Then, for any pair of marginals P^+, P^- where $y^+ \sim P^+(y^+)$ and $y^- \sim P^-(y^-)$, we have

$$\begin{aligned} \mathbb{E}[\Delta_t(y^+, y^-)] &= \mathbb{E}_{P^+}[r(x, y^+)] - \mathbb{E}_{P^-}[r(x, y^-)] \\ &\leq L \text{IPM}_{\mathcal{F}_1}(P^+, P^-) \leq L W_1(P^+, P^-) \\ \text{IPM}_{\mathcal{F}_1}(P^+, P^-) &= \sup_{f \in \mathcal{F}_1} \left(\mathbb{E}_{y^+ \sim P^+}[f(y^+)] - \mathbb{E}_{y^- \sim P^-}[f(y^-)] \right) \end{aligned} \quad (20)$$

where W_1 is the 1-Wasserstein distance.

Proof. By definition of IPM over 1-Lipschitz functions and r/L is admissible, the above inequality is the Kantorovich-Rubinstein duality IPM over 1-Lipschitz functions equals W_1 provided in [23]. In addition, although Lemma 5 requires r to be an L -Lipschitz function, we have observed

that a local L -Lipschitz reward function, which is satisfied in our setup, is also sufficient. Indeed, prior studies [34] rigorously derives bounds on the local Lipschitz constants of deep neural networks and shows they can be meaningfully controlled despite huge global constants. This result indicate that the LLMs behave smoothly around their high-probability outputs. In our context, we only need the log-ratio to be Lipschitz on the region visited by preference pairs, not globally over all possible outputs. Transformer-based LLMs incorporate norm control, weight decay, and normalization layers, which implicitly bound gradient magnitudes and curtail abrupt jumps in logits. Empirically, small semantic perturbations rarely cause extreme changes in logits, suggesting local smoothness holds on the data manifold [32, 105] Thus, a locally valid Lipschitz constant suffices the requirement of Lemma 5. Therefore, while LLMs may not be globally Lipschitz, they plausibly satisfy the needed local Lipschitz continuity in the regions relevant to DPO, making Lemma 5 still valid in practice.

In addition, it can be shown that $W_1(P^+, P^-) \leq 3W_1(\pi_t, \pi_{t-1})$ follows naturally from the triangle inequality of the Wasserstein distance. In particular, if the preference distributions P^+ and P^- remain close to the current and previous policies, respectively, such that $W_1(P^+, \pi_t) \leq W_1(\pi_t, \pi_{t-1})$ and $W_1(P^-, \pi_{t-1}) \leq W_1(\pi_t, \pi_{t-1})$, then we obtain

$$\begin{aligned} W_1(P^+, P^-) &\leq W_1(P^+, \pi_t) + W_1(\pi_t, \pi_{t-1}) + W_1(\pi_{t-1}, P^-) \\ &\leq 3W_1(\pi_t, \pi_{t-1}) \end{aligned} \quad (21)$$

This conditions are typically satisfied in the DPO training, where preference sampling is a monotone and non-expansive process, e.g., sampling candidates from a mixture (please refer to Remark 1 in Section A.2). In the context of continual learning of LMMs, the inequality $W_1(P^+, P^-) \leq 3W_1(\pi_t, \pi_{t-1})$ implies that the discrepancy between well-retained and forgotten knowledge is bounded by the overall policy shift between two learning steps. Intuitively, both P^+ and P^- remain anchored around their respective policies, so the overall variation between them is bounded by a constant multiple of the inter-policy shift $W_1(\pi_t, \pi_{t-1})$. Concurrently, both P^+ and P^- remain anchored around their respective policies— P^+ near the current policy π_t and P^- near the previous policy π_{t-1} —so if the model update between tasks is smooth, the semantic drift between memory retention and forgetting remains limited. This highlights that our continual DPO training enforces a stable adaptation process, where catastrophic forgetting is controlled by bounding the inter-policy Wasser-

stein distance.

Now, the inequality in Eqn. (20) can be further rewritten as follows:

$$\begin{aligned} \mathbb{E}[\Delta_t(y^+, y^-)] &= \mathbb{E}_{P^+}[r(x, y^+)] - \mathbb{E}_{P^-}[r(x, y^-)] \\ &\leq 3LW_1(\pi_t, \pi_{t-1}) \end{aligned} \quad (22)$$

Lemma 6 A Transport–Entropy Inequality. *Since the output probability $p(y|x)$ produced by the LMM of previous learning step π_{t-1} is computed based on the softmax on the logit scores of token y , we can view π_{t-1} as a Boltzmann distribution over token sequences. Then, without a strict argument, we assume that π_{t-1} satisfies the Talagrand $T_2(C_0)$ inequality [49, 97]:*

$$W_2^2(\mu, \pi_{t-1}) \leq 2C_0 D_{\text{KL}}(\mu \| \pi_{t-1}) \quad \text{for all } \mu, \quad (23)$$

Then, since $W_1 \leq W_2$, by substituting μ by π_t , we have the final inequality as follows:

$$W_1(\pi_t, \pi_{t-1}) \leq \sqrt{2C_0 D_{\text{KL}}(\pi_t \| \pi_{t-1})} \quad (24)$$

Proof. The proof of Talagrand $T_2(C_0)$ inequality has been shown in prior studies [9].

Proof of Lemma 1. From Lemmas 4-6, we have

$$\begin{aligned} \mathcal{L}_{\text{DPO}}(\theta; x) &\geq \log 2 - \frac{\beta}{2} \mathbb{E}[\Delta_t] \\ &\geq \log 2 - \frac{3\beta}{2} LW_1(\pi_t, \pi_{t-1}) \\ &\geq \log 2 - \frac{3\beta}{2} L \sqrt{2C_0 D_{\text{KL}}(\pi_t \| \pi_{t-1})} \\ \Rightarrow \log 2 - \mathcal{L}_{\text{DPO}}(\theta; x) &\leq \frac{3\beta L}{2} \sqrt{2C_0 D_{\text{KL}}(\pi_t \| \pi_{t-1})} \\ \Rightarrow D_{\text{KL}}(\pi_t \| \pi_{t-1}) &\geq \frac{(\log 2 - \mathcal{L}_{\text{DPO}}(\pi_t, \pi_{t-1}))^2}{\frac{1}{2}\beta^2 3^2 L^2 2C_0} \\ D_{\text{KL}}(\pi_t \| \pi_{t-1}) &\geq \frac{(\log 2 - \mathcal{L}_{\text{DPO}}(\pi_t, \pi_{t-1}))^2}{\beta^2 3^2 L^2 C_0} \end{aligned} \quad (25)$$

Then, assume that there exists a constant $M \geq 1$ such that for all (x, y) ,

$$\frac{1}{M} \leq \frac{\pi_{t-1}(y|x)}{\pi_t(y|x)} \leq M. \quad (26)$$

This ensures that the predicted distributions of the LMM model at the previous learning step π_{t-1} and the current learning step π_t are mutually absolutely continuous and that their density ratio is uniformly bounded. In other words, it prevents the predictions of the LMM from collapsing across consecutive learning steps, ensuring a stable and smooth evolution of the output distribution during the continual learning procedure. Let $h(x, y) = \frac{\pi_{t-1}(y|x)}{\pi_t(y|x)}$ denote the likelihood ratio. The forward and reverse KL divergence can be rewritten as follows

$$D_{\text{KL}}(\pi_{t-1} \| \pi_t) = \mathbb{E}_{(x,y) \sim \pi_t} [h(x, y) \log h(x, y)], \quad (27)$$

$$D_{\text{KL}}(\pi_t \| \pi_{t-1}) = \mathbb{E}_{(x,y) \sim \pi_t} [-\log h(x, y)], \quad (28)$$

where $h(x, y) = \frac{\pi_{t-1}(y|x)}{\pi_t(y|x)}$.

Lower bound of $D_{\text{KL}}(\pi_{t-1} \| \pi_t)$. The function $f(u) = u \log u$ is convex with $f''(u) = 1/u$. On the interval $[1/M, M]$, the smallest curvature is $1/M$. By the second-order convexity bound around $u = 1$,

$$u \log u \geq (u - 1) + \frac{1}{2M}(u - 1)^2. \quad (29)$$

Since $\mathbb{E}_{x,y \sim \pi_t(y|x)} [h(x, y) - 1] = 0$, taking the expectation under π_t will result in

$$D_{\text{KL}}(\pi_{t-1} \| \pi_t) \geq \frac{1}{2M} \mathbb{E}_{\pi_t} [(h(x, y) - 1)^2]. \quad (1)$$

Upper bound of $D_{\text{KL}}(\pi_t \| \pi_{t-1})$. Similarly, with $g(u) = -\log u$, we have $g''(u) = 1/u^2$, and on $[1/M, M]$, the largest curvature is M^2 . Hence,

$$-\log u \leq (1 - u) + \frac{M^2}{2}(u - 1)^2. \quad (30)$$

Then, taking expectation under π_t will result in

$$D_{\text{KL}}(\pi_t \| \pi_{t-1}) \leq \frac{M^2}{2} \mathbb{E}_{\pi_t} [(h(x, y) - 1)^2]. \quad (31)$$

From Eqn. (1) and and Eqn. (30), we can obtain

$$D_{\text{KL}}(\pi_{t-1} \| \pi_t) \geq \frac{1}{M^3} D_{\text{KL}}(\pi_t \| \pi_{t-1}). \quad (32)$$

Then, let us define $c = M^3$. Eqn. (25) can be further derived as follows:

$$\begin{aligned} D_{\text{KL}}(\pi_{t-1} \| \pi_t) &\geq \frac{(\log 2 - \mathcal{L}_{\text{DPO}}(\theta; x))^2}{c\beta^2 3^2 L^2 C_0} \\ &\geq \frac{1}{C_{\text{lower}}} (\log 2 - \mathcal{L}_{\text{DPO}}(\theta; x))^2 \end{aligned} \quad (33)$$

where $C_{\text{lower}} = c\beta^2 3^2 L^2 C_0$.

A.2. Proof of Lemma 2

Remark 1. Mixture Sampling and Monotone Labeling. For each prompt x , the output candidates are sampled from

$$Q_x = \alpha \pi_{t-1}(\cdot | x) + (1 - \alpha) \pi_t(\cdot | x) \quad \text{with } \alpha \in (0, 1], \quad (34)$$

and the selection kernel (human or reward model) chooses the preferred/dispreferred outputs (y^+, y^-) *monotonically* with the underlying reward, inducing pair marginals P_x^+, P_x^- that do not expand total variation beyond what is present in Q_x . Formally, we have

$$\text{TV}(\pi_{t-1}(\cdot | x), \pi_t(\cdot | x)) \leq \frac{1}{\alpha} \text{TV}(P^+, P^-). \quad (35)$$

Remark 1 is both natural and theoretically justified in the context of continual learning via DPO. The candidate

responses of DPO are typically drawn from a mixture of the previous and current policies, Q_x , to ensure balanced exposure to both past and newly adapted behaviors. The monotone labeling condition further indicates that the preference signal, whether derived from humans or a reward model, preserves the true reward ordering of outputs. Then, the total-variation inequality then follows from the data-processing principle, i.e., applying a monotone labeling kernel cannot increase statistical divergence between distributions. Intuitively, the preference selection process can only reveal discrepancies already present in the mixture Q_x , not amplify them. Consequently, Remark 1 enforces a bounded relationship between the divergence of the induced pairwise marginals (P_x^+, P_x^-) and the divergence between the underlying policies (π_{t-1}, π_t) . In addition, this guarantees that updates to π_t remain geometrically close to π_{t-1} , providing a stability-adaptability balance in the continual learning setting, i.e., the model can adapt to new data or tasks while preventing catastrophic forgetting.

Remark 2. Sign Consistency. The predictor π_t is *Bayes-consistent in sign* on the support of $M_x := \frac{1}{2}(P_x^+ + P_x^-)$:

$$\text{sgn}(q_\theta(z) - \frac{1}{2}) = \text{sgn}(\eta(z) - \frac{1}{2}) \quad \text{for } M_x\text{-a.e. } z,$$

where $\eta(z) = \frac{dP_x^+}{d(P_x^+ + P_x^-)}(z)$ and $q_\theta(z) = \sigma(\beta s_\theta(z))$ with $\sigma(u) = \frac{1}{1+e^{-u}}$. This remark is standard in excess-risk calibration and holds whenever the logistic excess risk is sufficiently small to ensure boundary consistency.

Lemma 7 Logistic Calibration for Pairs. Given P^+ and P^- , the total variation of $TV(P^+, P^-)$ will be bounded by the DPO loss:

$$TV(P^+, P^-) \leq 2\sqrt{2} \sqrt{\mathcal{L}_{\text{DPO}}(\pi_t, \pi_{t-1}) - \mathcal{L}_{\text{DPO}}^*(\pi_t, \pi_{t-1})} \quad (36)$$

where $\mathcal{L}_{\text{DPO}}^*(\pi_t, \pi_{t-1})$ is the Bayes-optimal logistic pairwise loss.

Proof. Let us abbreviate $P^+ = P_x^+$, $P^- = P_x^-$, and $M = \frac{1}{2}(P^+ + P^-)$. The DPO loss and its Bayes-optimal counterpart can be written as

$$\begin{aligned} \mathcal{L}_{\text{DPO}}(\pi_t, \pi_{t-1}) &= \mathbb{E}_{Z \sim M}[\text{CE}(\eta(Z), q_\theta(Z))] \\ \mathcal{L}_{\text{DPO}}^*(\pi_t, \pi_{t-1}) &= \mathbb{E}_{Z \sim M}[\text{CE}(\eta(Z), \eta(Z))] \end{aligned} \quad (37)$$

where $\text{CE}(\cdot, \cdot)$ is the binary cross-entropy function, $\eta(\cdot)$ represents the true (Bayes-optimal) preference probability between positive and negative outcomes, $q_\theta(Z)$ is model-predicted probability obtained from the logit margin of the LMM model. Then, the excess DPO risk is formed as:

$$\begin{aligned} \mathfrak{R}_{\pi_t, \pi_{t-1}}(x) &= \mathcal{L}_{\text{DPO}}(\pi_t, \pi_{t-1}) - \mathcal{L}_{\text{DPO}}^*(\pi_t, \pi_{t-1}) \\ &= \mathbb{E}_{Z \sim M}[\text{KL}(\text{Bern}(\eta(Z)) \parallel \text{Bern}(q_\theta(Z)))]. \end{aligned} \quad (38)$$

where Bern is the Bernoulli distribution.

Bernoulli Pinsker Inequality. For any z , Pinsker’s inequality for Bernoulli distributions gives

$$\text{KL}(\text{Bern}(\eta(z)) \parallel \text{Bern}(q_\theta(z))) \geq 2(\eta(z) - q_\theta(z))^2. \quad (39)$$

Hence,

$$\mathbb{E}_M[(\eta - q_\theta)^2] \leq \frac{1}{2} \mathfrak{R}_{\pi_t, \pi_{t-1}}(x). \quad (40)$$

Sign Consistency Implies Margin Control. Under Remark 2, since η and q_θ lie on the same side of $\frac{1}{2}$ for almost every z :

$$\begin{aligned} |\eta(z) - \frac{1}{2}| &\leq |\eta(z) - q_\theta(z)| + |q_\theta(z) - \frac{1}{2}| \leq 2|\eta(z) - q_\theta(z)| \\ &\Rightarrow |2\eta(z) - 1| \leq 4|\eta(z) - q_\theta(z)| \end{aligned} \quad (41)$$

By definition of total variation, we have

$$TV(P^+, P^-) = \mathbb{E}_{Z \sim M}[|2\eta(Z) - 1|]. \quad (42)$$

Then, applying Eqn. (41) and Cauchy-Schwarz, we will receive

$$TV(P^+, P^-) \leq 4 \mathbb{E}_M |\eta - q_\theta| \leq 4 \sqrt{\mathbb{E}_M (\eta - q_\theta)^2}. \quad (43)$$

Then, substitute Eqn.(40) will result in

$$\begin{aligned} TV(P^+, P^-) &\leq 4 \sqrt{\frac{1}{2} \mathfrak{R}_{\pi_t, \pi_{t-1}}(x)} \\ &= 2\sqrt{2} \sqrt{\mathcal{L}_{\text{DPO}}(\pi_t, \pi_{t-1}) - \mathcal{L}_{\text{DPO}}^*(\pi_t, \pi_{t-1})}. \end{aligned} \quad (44)$$

Proof of Lemma 2. By Pinsker’s inequality, we have

$$\begin{aligned} TV(\pi_{t-1}, \pi_t) &\leq \sqrt{\frac{1}{2} D_{\text{KL}}(\pi_{t-1} \parallel \pi_t)}, \\ \Rightarrow D_{\text{KL}}(\pi_{t-1} \parallel \pi_t) &\leq 2 TV(\pi_{t-1}, \pi_t)^2. \end{aligned} \quad (45)$$

Then, substituting Remark 1 and Lemma 7 into Pinsker’s relation will result in

$$\begin{aligned} D_{\text{KL}}(\pi_{t-1} \parallel \pi_t) &\leq 2 \left(\frac{2\sqrt{2}}{\alpha} \sqrt{\mathcal{L}_{\text{DPO}}(\pi_t, \pi_{t-1}) - \mathcal{L}_{\text{DPO}}^*(\pi_t, \pi_{t-1})} \right)^2 \\ &\leq \frac{16}{\alpha^2} (\mathcal{L}_{\text{DPO}}(\pi_t, \pi_{t-1}) - \mathcal{L}_{\text{DPO}}^*(\pi_t, \pi_{t-1})) \\ &\leq \frac{16}{\alpha^2} \mathcal{L}_{\text{DPO}}(\pi_t, \pi_{t-1}) \\ &= C_{\text{upper}} \mathcal{L}_{\text{DPO}}(\pi_t, \pi_{t-1}) \end{aligned} \quad (46)$$

where $C_{\text{upper}} = \frac{16}{\alpha^2}$.

A.3. Proof of Lemma 3

Proof. Since $\log p \leq 0$, one has $0 \leq \alpha_\gamma(p) \leq (1-p)^\gamma$, and $(1-p)^\gamma \rightarrow 0$ exponentially as $\gamma \rightarrow \infty$. Then, for any fixed $p \in (0, 1)$, we have $\lim_{\gamma \rightarrow \infty} \alpha_\gamma(p) = 0$. As a result,

for each group k , if $p(z) \in (0, 1)$ a.s. and $\mathbb{E}[\|(p_\theta - 1)\nabla s_\theta\| | G_k] < \infty$, then $\lim_{\gamma \rightarrow \infty} w_k^\gamma(\theta) = 0$. By definition, we have

$$\|B_\gamma(\theta)\| \leq \sum_{k=1}^K |q_k - q'_k| |w_k^\gamma(\theta)| \|m_k(\theta)\|. \quad (47)$$

Since $w_k^\gamma(\theta) \rightarrow 0$ for each k as $\gamma \rightarrow \infty$, the sum tends to 0.

B. DPO Data

B.1. Data Description

We share a part of our data in the supplementary submission. Due to the file size limitations of the supplementary submission, we provide only a partial subset of the dataset used in our experiments. This subset is intended to illustrate the data structure, annotation format, and representative visual characteristics. The **full dataset**, including all images and finalized annotations, will be released publicly upon acceptance of the paper.

B.2. Copyright and Usage Notice

All images included in this supplementary package remain the intellectual property of their original creators and data sources. We do not claim copyright over any raw images provided here. The images are included solely for scientific reference and reproducibility under fair-use guidelines.

In the final version of the dataset, we will release the complete annotations produced in this work while preserving the copyright of all images. Access to the full image collection will be provided in accordance with the licensing and usage terms of the original datasets. Users of this supplementary material are responsible for ensuring that any use of these images complies with the corresponding copyright requirements.